Simulation-based travel time reliable signal control

Chen, X; Osorio, C.; Santos, Bruno F.

DOI
10.1287/trsc.2017.0812

Publication date
2019

Document Version
Accepted author manuscript

Published in
Transportation Science

Simulation-based travel time reliable signal control

Carolina Osorio
Department of Civil and Environmental Engineering, Massachusetts Institute of Technology (MIT), Cambridge, MA02139, USA, osorioc@MIT.EDU,

Xiao Chen
School of Highway, Chang'an University, China, xiaochen@chd.edu.cn,

Bruno Filipe Santos
Department of Control and Operations, Faculty of Aerospace Engineering, Delft University of Technology, Delft 2600, Netherlands, B.F.Santos@tudelft.nl,

1. Introduction

Most urban transportation optimization problems are formulated based on first-order moments of network performance (e.g. expected trip travel times, expected throughput). Formulations based on the use of higher-order information can lead, for instance, to enhanced network reliability and enhanced network robustness. Enhancing the reliability of transportation networks is currently recognized as a critical goal by major transportation agencies. A Transport for London report identifies trip travel time reliability improvements as their primary objective (Transport for London 2010). U.S. reports have also emphasized the importance of improving the reliability of our transportation systems (Texas Transportation Institute 2012, Department of Transportation 2008).

Problem formulations that account for higher-order distributional information are rare and are usually based on the use of low-resolution analytical models. Nonetheless, providing an analytical, let alone tractable, approximation of the distribution of the main network performance measures is a major challenge (see for instance, Osorio and Flötteröd (2014), Peterson et al. (1995), Odoni and Roth (1983)), and is often achieved by simplifying, or even omitting, spatial-temporal dependencies. Stochastic simulation-based models can yield distributional estimates that account for such intricate dependencies. Nonetheless, the efficient use of simulation-based higher-order information for optimization has yet to be explored. This paper contributes to address the following question: how can simulation-based higher-order distributional information be efficiently used for network optimization?

This paper focuses on travel time reliability problems. For a description of other network reliability metrics, see Clark and Watling (2005). The two most common metrics used to address travel

time reliability are trip travel time variability and trip travel time percentiles (e.g., 95^{th} percentile) (OECD 2010). A major challenge in improving travel time reliability is the approximation of the network travel time distribution. An analytical and accurate expression for the full joint network distribution is difficult to derive given the intricate between-link spatial-temporal dependencies. A variety of analytical approximations have been proposed based on distributional assumptions ranging from: 1) knowledge of the functional form of the full joint network distribution (Mirchandani and Soroush 1987); 2) knowledge of the functional form of the marginal link distributions (Fu and Hellinga 2000); 3) knowledge of moments of the marginal link distributions (Ng et al. 2011). Empirical (non-parametric) analysis of link travel time distributions have also been proposed (van Lint and van Zuylen 2005, Chen et al. 2003). This paper uses simulated travel time distributional estimates. The estimates are obtained from detailed stochastic microscopic traffic simulators that account for intricate vehicle-to-vehicle and vehicle-to-infrastructure interactions.

This paper focuses on reducing travel time variability. In general, spatial-temporal variations in both demand and supply can lead to increased variability (see Clark and Watling (2005) or Noland and Polak (2002) for details on common underlying causes of supply and demand variability). Increased variability leads to increased uncertainty for travelers, and increased travel cost (Noland and Polak 2002). There is a substantial body of research that studies the behavioral impacts of travel time variability. Noland and Polak (2002) provide a review. Carrion and Levinson (2012) review methodologies to quantify the value of travel time reliability. Such studies highlight that travel time variability is accounted for by travelers in numerous travel decisions, and that its reduction is of high value to travelers. Thus, there is a need to design and operate transportation systems such as to mitigate it.

The optimization problems considered in this paper are travel time reliable traffic signal control problems. The importance of accounting for travel time variability in signal control has been emphasized by Yin (2008). The traditional signal control objectives are network efficiency maximization, such as expected throughput maximization (Abu-Lebdeh and Benekohal 1997), or minimization of expected travel time (Osorio and Chong 2015), of the expected number of vehicle stops or of expected delay (Wong et al. 2002).

To the best of our knowledge, the few studies that have accounted for travel time variability in the design of signal plans are based on analytical methods. Yin (2008) proposes an analytical technique to reduce the standard deviation of delay and, ultimately, enhance the robustness of signal plans to fluctuations in demand. The demand fluctuation is represented by different demand scenarios. The technique is applied to an isolated intersection. Zhang et al. (2010) extend the work of Yin (2008) to account for multiple intersections along an arterial. Another extension is proposed by Li (2011), which illustrates the method on an isolated intersection. Park and Kamarajugadda (2007) and

Kamarajugadda and Park (2003) develop an analytical approximation of delay variance. Parametric distributions are assumed for link volumes and the corresponding parameters are estimated with traffic count data. The analytical delay variances are then used to address a signal control problem for an isolated intersection and then for a set of two adjacent intersections. This analytical approach is not designed for use within a general topology network.

Analytical techniques are computationally tractable and efficient, yet rely on strong distributional assumptions, such as the choice of a given parametric distribution for link or path delay. The use of stochastic simulators allows for more flexible and realistic assumptions that can contribute to capture the intricate form that the travel time distribution may take (e.g., multi-modal distribution).

This paper uses a class of urban traffic simulation models known as stochastic microscopic simulators. The proposed methodology is suitable for any type of computationally inefficient simulation-based traffic model (e.g., macroscopic, mesoscopic or microscopic; deterministic or stochastic, etc.). For a review of traffic simulation models, see Barceló (2010). Of the three main families of simulation models (macroscopic, mesoscopic and microscopic), microscopic models embed the most detailed representation of both demand and supply. They explicitly represent individual vehicles and can account for vehicle-specific technologies/attributes. They also represent individual travelers and embed detailed disaggregate behavioral models (e.g. response to en-route traffic information, departure-time choice, route choice, lane-changing, car-following). They provide a detailed representation of the underlying supply network (e.g. variable message signs, public transport priorities). Thus, these traffic simulators can describe in detail the interactions between vehicle performance (e.g., instantaneous energy consumption, emissions), traveler behavior and the underlying transportation infrastructure, and yield a detailed description of traffic dynamics in urban networks. Since they account for intricate local traffic dynamics and demand-supply interactions, they capture the between-link spatial-temporal dependencies of the main performance measures, and can thus yield accurate estimates of the full distribution of the main performance measures. These simulators are suitable tools to design traffic management strategies that enhance travel time reliability, and more generally network reliability.

The computational inefficiency of microscopic simulators has mostly limited their use to what-if (i.e., scenario-based) analysis (as in, for instance, Bullock et al. (2004), Ben-Akiva et al. (2003)). Their use within simulation-based optimization (SO) algorithms is rare, and is limited to the use of first-order distributional information (Osorio and Selvam 2017, Osorio and Nanduri 2015a,b, Osorio and Chong 2015, Li, Abbas, Pasupathy and Head 2010, Stevanovic et al. 2009, 2008, Branke et al. 2007, Yun and Park 2006, Hale 2005, Joshi et al. 1995). This paper proposes a methodology that

enables the use of high-resolution stochastic traffic simulators to efficiently address higher-order SO problems.

We consider signal control problems for congested urban networks and address large-scale problems. The simulated travel time distributional estimates are embedded within a simulation-based optimization (SO) algorithm and are used to identify signal plans with reduced expectation and standard deviation of travel time metrics. By using simulated distributional estimates, the proposed approach accounts for intricate spatial-temporal fluctuations in demand-supply interactions, leading to intricate within-time-of-day travel time variabilities.

Given the computational inefficiency of stochastic microscopic simulators, this paper focuses on the development of computationally efficient SO techniques. We consider tight computational budgets, which are defined as a maximum (and small) number of simulation runs. The objective is to identify within this budget signal plans that improve first- and second-order distributional information, and do so at the city-scale. In order to achieve efficiency, information from the (inefficient) simulator is coupled with information from an efficient (i.e. tractable and differentiable) analytical approximation of the objective function. The role of the simulator is to provide a highly detailed approximation of the distributions of interest, whereas that of the analytical model is to provide structural information to the SO algorithm, enhancing its efficiency. This paper formulates a tractable analytical approximation of the simulation-based higher-order performance metrics, this analytical approximation is embedded within the SO algorithm and is used to enhance the computational efficiency of the SO algorithm.

To the best of our knowledge, this paper constitutes the first to: 1) use higher-order distributional information from stochastic simulators to solve transportation optimization problems, 2) use higher-order distributional information, analytical or simulation-based, to solve large-scale signal control problems, and 3) enable higher-order simulation-based transportation optimization problems to be solved in a computationally efficient way. In particular, the problem addressed in Section 3.3 is considered a large-scale traffic signal control problem, as well as a difficult high-dimensional simulation-based optimization problem.

Section 2 presents the proposed methodology. Section 3 applies the methodology to two case studies: the Lausanne city center and the full city network. Section 4 presents the main conclusions and discusses areas of ongoing and future research. The Appendix contains: the formulation of the analytical network models used as part of the SO framework (Section 5), the SO algorithm (Section 6) and the formulation of the optimization problem solved at every iteration of the SO algorithm (Section 7).

2. Methodology

Section 2.1 describes the general SO framework of this paper. The reliable simulation-based signal control problem is formulated in Section 2.2. The SO algorithm uses an analytical approximation of the simulation-based objective function derived from analytical network models. These analytical approximations are derived in Sections 2.3 and 2.4. Section 2.5 summarizes the proposed methodology.

2.1. Simulation-based optimization framework

For reviews of SO methods, see Hachicha et al. (2010), Barton and Meckesheimer (2006) and Fu et al. (2005). We use the SO framework proposed by Osorio and Bierlaire (2013). This section briefly presents the framework. For details regarding its formulation, we refer the reader to Osorio and Bierlaire (2013). The formulation of the method has been extended to successfully address difficult constrained simulation-based problems in a computationally efficient manner (Osorio and Nanduri 2015a,b, Osorio and Chong 2015, Osorio and Selvam 2017, Zhang et al. 2017).

This algorithm can address continuous nonlinear generally constrained optimization problems where the objective function is derived from a stochastic simulator, i.e. a closed-form expression is not available for the objective function, whereas closed-form analytical expressions are available for all constraints. Such problems can be formulated as:

$$\min_{x} f(x, z; p) \tag{1}$$

subject to

$$g(x, z; p) = 0. \tag{2}$$

The feasible space is defined by g which is a set of general, typically non-convex, deterministic, analytical and differentiable constraints. The objective function f can be, for instance, the expected value of a given stochastic performance measure G: $f(x, z; p) = E[G(x, z; p)]$. The decision vector x is real-valued (e.g., green splits), z denotes other endogenous simulation variables (e.g., departure-time/mode/route choice probabilities), and p denotes the deterministic exogenous simulation parameters (e.g., network topology).

This SO method is a metamodel method. A metamodel is an analytical approximation of the objective function f. The main ideas of metamodel SO methods are illustrated in Figure 1. At a given iteration k, the SO algorithm iterates over the following steps. First, determine what point, among the points simulated so far, has the best performance. This point is denoted x_k and is known as the current iterate. Second, fit the metamodel, m_k, based on the set of simulation observations collected so far. The metamodel parameter vector is denoted β_k. Use m_k to perform optimization

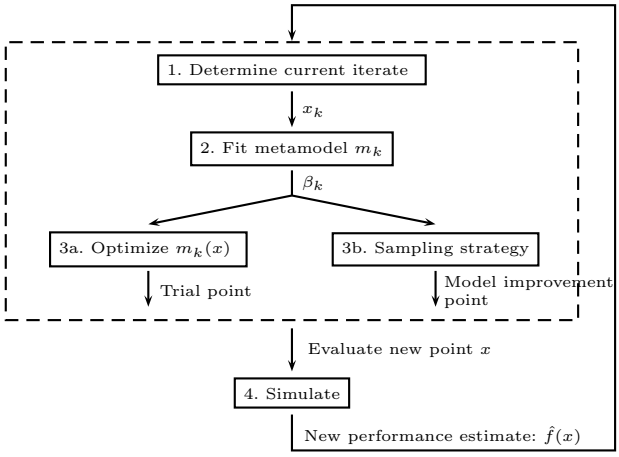

Figure 1 Metamodel simulation-based optimization methods (Chong and Osorio 2017).

and derive a trial point (step 3a). An optional step, which not all SO algorithms embed, is step 3b. In this step, points that may not be solutions to the metamodel optimization problem are simulated. These points are known as model improvement points. Step 4 evaluates via simulation the performance of the new points (the trial point and any model improvement points). Step 4 leads to new simulation observations. As new simulated observations become available, the accuracy of the metamodel can be improved (Step 2), leading to trial points with improved performance (Step 3a). These steps are iterated until, for instance, the computational budget is depleted. The SO algorithm is given in detail in the Appendix (Section 6).

At every iteration of the SO algorithm, the metamodel optimization problem is solved (step 3a). The main idea of the metamodel optimization problem is to replace the (unknown) simulation-based objective function (Equation 1) with the analytical metamodel function, m, such that efficient deterministic optimization techniques can be used. A detailed formulation of the metamodel optimization problem of this paper is given in the Appendix (Section 7). Reviews of metamodels are given by Conn et al. (2009b), Barton and Meckesheimer (2006) and Søndergaard (2003). Metamodels are classified in the literature as either physical or functional metamodels (Søndergaard 2003, Serafini 1998). Physical metamodels consist of application-specific metamodels, their functional form and parameters have a physical or structural interpretation. Functional metamodels are general-purpose (i.e. generic) functions that are chosen based on their analytical tractability but do not take into account any information with regards to the specific objective function, let alone the structure of the underlying problem.

The Osorio and Bierlaire (2013) framework proposes a metamodel that combines a functional and a physical component and has the following form:

$$m(x, y; \alpha, \beta, q) = \alpha f_A(x, y; q) + \phi(x; \beta), \tag{3}$$

where ϕ denotes the functional component, f_A (the physical component) represents the approximation of the objective function (f of Equation (1)) as derived by an analytical macroscopic traffic model, y are endogenous macroscopic model variables (e.g., queue-length distributions), q are exogenous macroscopic parameters (e.g., total demand), α and β are parameters of the metamodel. The metamodel is fitted based on simulation observations of the objective function via regression. At each iteration, the simulator and the queueing model are evaluated at a set of points, and then the metamodel is fitted by solving a least squares problem based on both the current iteration simulation observations and all the previous simulation observations.

The functional component ϕ is defined as a quadratic polynomial in x with diagonal second-derivative matrix:

$$\phi(x;\beta) = \beta^1 + \sum_{j=1}^{d} \beta^{j+1} x^j + \sum_{j=1}^{d} \beta^{j+d+1} (x^j)^2, \tag{4}$$

where d is the dimension of x, x^j and β^j are the j^{th} components of x and β, respectively.

The physical component f_A is derived by evaluating an analytical macroscopic traffic model, which is referred to as the auxiliary traffic model. It provides a problem-specific approximation of the objective function, i.e. its functional form will depend on the underlying problem formulation. It also provides a global approximation of the objective function (i.e., an approximation across the entire feasible region). The metamodel is therefore a linear combination of an analytical global and problem-specific approximation of the objective function and a quadratic error term.

In this paper, the physical component is an analytical and differentiable macroscopic traffic model formulated based on probabilistic finite capacity queueing network theory. It provides structural information about the problem at hand. It enables the identification of well performing alternatives (e.g. trial points) with very small samples (i.e. good short-term algorithmic performance). The use of an auxiliary model that is probabilistic allows us to address problems that are formulated based on higher-order (i.e., beyond first-order) distributional information.

As stated above, at every iteration of the SO algorithm, the metamodel optimization problem is solved (step 3a of Figure 1). This problem is also referred to as the trust region subproblem. When using a macroscopic traffic model as the physical component of the metamodel, the subproblem solved at every iteration is constrained by the macroscopic traffic model. For this subproblem to be solved efficiently, it is necessary to use a macroscopic model that is both: (i) scalable, such that problems for large-scale networks can be addressed, and (ii) computationally efficient, such that the subproblem can be solved fast. The macroscopic models used in this paper achieve both of these goals. Their full formulation is given in the Appendix (Sections 5.1 and 5.2). First, they are both computationally efficient because they are defined as a differentiable system of nonlinear equations, which can be evaluated with a variety of standard numerical techniques. Second, they

are both scalable: the dimension of the system of equations scales linearly with the number of links in the network and is independent of the space capacity of the links in the network. The proposed framework can be used with any other macroscopic model that is scalable and efficient.

2.2. Reliable signal control problem

The most common approach to account for both expected travel time and travel time variability information is to use a linear combination: $t_E + rt_V$, where t_E denotes the expected trip travel time, t_V denotes a measure of trip travel time variability, and r is a weight parameter known as the reliability ratio. The reliability ratio is defined as the marginal rate of substitution between expected travel time and travel time reliability (Carrion and Levinson 2012). The value of the reliability ratio can vary according to, for instance, the network, the time-of-day or the trip purpose. In practice, travel time and travel time variability valuation studies based on travel surveys are carried out in order to obtain an estimate for r. This linear combination approach is used in various studies, such as in Yin (2008) and in the traditional "mean-variance" approach (Jackson and Jucker 1982).

Often, the variability metric t_V consists of the trip travel time standard deviation. The objective function of this paper follows that same functional form, i.e., we combine expectation and standard deviation information of a given travel time performance metric. The travel time metric used is the total link travel time, i.e., the sum of travel times over all links in the area/network of interest. Link travel time metrics are easier to both measure in the field and to approximate analytically, compared to trip travel time metrics. Link metrics are also more suitable metrics when controlling a small area within a larger network (e.g. a small set of intersections within a full city).

We consider a fixed-time signal control problem, where the decision variables are the green splits. In this problem, the stage structure is given, the offsets, the cycle times and the all-red durations are fixed. For a more detailed description of this terminology see Osorio (2010, Section 4.2.2 and Appendix A). Fixed-timed plans are determined offline. They are traditional control strategies that do not exploit real-time traffic data. They are broadly used in many cities with a low, or inexistent, deployment of traffic sensors. For cities with abundant real-time traffic data, fixed-time plans are often chosen for areas where congestion is both high and uniformly distributed, such as in New York City (Osorio et al. 2015) or for areas with intricate network topologies (e.g., grid topologies).

The choice of green splits as the decision vector is based on insights obtained as part of our collaboration with the New York City Department of Transportation (NYCDOT). For many fixed-time controlled intersections within Manhattan, the main variables regularly updated are the green splits. More general problem formulations, can also optimize the offsets, which can lead to performance improvements through enhanced coordination between adjacent intersections and the stage structure. A discussion of these extensions is given in Section 4.

In order to formulate the problem, we introduce the following notation:

T_i	Travel time along link i;
$x(j)$	green split of phase j;
x_L	vector of minimal green splits;
a_i	available cycle time of intersection i;
c_i	cycle time of intersection i;
$\mathscr{L}$	set of links within the area of interest;
$\mathscr{Q}$	set of queues that represent the links of $\mathscr{L}$;
$\mathscr{I}$	set of intersection indices;
$\mathscr{P}_I(i)$	set of phase indices of intersection i;
r	reliability ratio.

The signal control problem is formulated as follows:

$$\min_x f(x,z;p) = E[\sum_{i\in\mathscr{L}} T_i(x,z;p)] + rSD[\sum_{i\in\mathscr{L}} T_i(x,z;p)], \tag{5}$$

subject to

$$\sum_{j\in\mathscr{P}_I(i)} x(j) = \frac{a_i}{c_i},\ \forall i \in \mathscr{I} \tag{6}$$

$$x \geq x_L. \tag{7}$$

The performance metric used, $\sum_{\mathscr{L}} T_i$, is the total link travel time. Hereafter, we no longer indicate the dependence of T_i on x, z and p. The objective function of this problem (Equation (5)) consists of a linear combination of the expected total link travel time, $E[\sum_{\mathscr{L}} T_i(x,z;p)]$, and the standard deviation of total link travel time $SD[\sum_{\mathscr{L}} T_i(x,z;p)]$. Constraints (6) guarantee that for a given intersection the sum of green splits of the endogenous phases equals the available cycle time. Constraints (7) correspond to the lower bound value for the green splits. In the case studies of this paper it is set to 4 seconds following Swiss transportation norms (VSS 1992).

For the case studies of this paper (Section 3), the simulators used are stochastic dynamic microscopic traffic models. The dynamic traffic assignment is based on the use of a stochastic C-logit route choice model (Cascetta et al. 1996). The deterministic part of the route choice utility function depends only on travel times. When evaluating via simulation the performance of a given signal plan (this is done at every iteration of the SO algorithm), the route travel times change in response to signal plan changes. This leads to changes in the route choice probabilities. In other words, the traffic assignment is endogenous and varies as a function of the signal plans. This is a suitable representation of the route choice behavior observed in practice. For a comparative study of user equilibrium, stochastic user equilibrium and system optimum assignments, see, for instance, Prashker and Bekhor (2000).

2.3. Physical component

Recall that the metamodel formulation of Equation (3) requires an analytical expression for f_A, which is the approximation of the objective function f (Equation (5)) as derived by the auxiliary traffic model. This section derives the analytical (and differentiable) approximation of the two components of f provided by the auxiliary traffic model. That is, we derive analytical approximations for $E[\sum_{\mathscr{L}} T_i]$ and for $SD[\sum_{\mathscr{L}} T_i]$; or equivalently $E[\sum_{\mathscr{Q}} T_i]$ and $SD[\sum_{\mathscr{Q}} T_i]$.

The auxiliary model used is an analytical queueing network model based on finite capacity queueing theory. Each lane in the road network is modeled as one (or a set of) queues. Each queue of the model is a finite capacity $M/M/1/k$ queue. The model is based on a stationary regime assumption. It consists of a system of nonlinear equations that relate the arrival and service rates of a queue to the demand and supply of its upstream and downstream queues. It describes spillbacks through the queueing theory notion of *blocking*. The model is suitable for large-scale analysis, as mentioned above, it's complexity is linear in the number of links in the network and is independent of the links space capacity. We briefly recall the main variables and parameters that define each queue. For a given queue i, we use the following notation.

λ_i	arrival rate;
$\hat{\mu}_i$	effective service rate (accounts for both service and eventual blocking);
k_i	space capacity;
N_i	number of vehicles in queue i;
$P(N_i = k_i)$	probability of queue i being full, also known as the blocking or spillback probability;
ρ_i	traffic intensity (defined as the ratio of arrival rate and effective service rate).

The queueing variables are related to the signal plans as defined by Equation (43) (in Appendix 7). This equation states that for a given lane its service rate is defined as the proportion of time (during a signal cycle) it has a green signal multiplied by the saturation rate. This proportion of time is the sum of the endogenous green splits (i.e., the decision variables of the signal control problem) and any fixed (exogenous) green time.

2.3.1. Expected total travel time The expected total travel time is obtained by summing the expected travel times of the queues (or equivalently links) of interest:

$$E[\sum_{i\in\mathscr{Q}} T_i] = \sum_{i\in\mathscr{Q}} E[T_i]. \tag{8}$$

The expected travel time of a given queue i is derived by applying Little's law (Little 2011, 1961):

$$E[T_i] = \frac{E[N_i]}{\lambda_i(1 - P(N_i = k_i))}, \tag{9}$$

where the expected queue-length of queue i, $E[N_i]$, is derived in Osorio and Chong (2015) and is given by:

$$E[N_i] = \rho_i \left(\frac{1}{1-\rho_i} - (k_i+1)\frac{\rho_i^{k_i}}{1-\rho_i^{k_i+1}} \right). \tag{10}$$

2.3.2. Total travel time standard deviation We now describe the approximation for $SD[\sum_{\mathcal{Q}} T_i]$. By definition:

$$SD[\sum_{\mathcal{Q}} T_i] = \sqrt{VAR[\sum_{\mathcal{Q}} T_i]}. \tag{11}$$

In order to derive a tractable analytical expression, we make the following approximation:

$$Var[\sum_{i\in\mathcal{Q}} T_i] \approx \sum_{i\in\mathcal{Q}} Var[T_i]. \tag{12}$$

The latter expression is exact only if all queues have independent travel times. This may be an inaccurate approximation in various congestion regimes. Nonetheless, recall that the main role of the physical component is to provide a tractable approximation of the objective function. Given the difficulty of accurately modeling between-link dependencies while preserving tractability (Osorio and Yamani 2014, Flötteröd and Osorio 2017, Osorio and Wang 2017), this independence approximation ensures tractability. By definition:

$$Var[T_i] = E[T_i^2] - E[T_i]^2. \tag{13}$$

Equation (9) gives the expression for $E[T_i]$. An expression for $E[T_i^2]$ is derived in Section 2.4 and is given by:

$$E[T_i^2] = \frac{1}{\hat{\mu_i}^2}\left(\frac{4\rho_i - 2\rho_i^2}{(1-\rho_i)^2} - \frac{2k_i\rho_i^{k_i+1}}{(1-\rho_i^{k_i})(1-\rho_i)} + \frac{2-(k_i+1)(k_i+2)\rho_i^{k_i}}{1-\rho_i^{k_i}}\right). \tag{14}$$

$Var[T_i]$ is therefore given by:

$$\begin{aligned} Var[T_i] = \frac{1}{\hat{\mu_i}^2}\left(\frac{4\rho_i - 2\rho_i^2}{(1-\rho_i)^2} - \frac{2k_i\rho_i^{k_i+1}}{(1-\rho_i^{k_i})(1-\rho_i)} + \frac{2-(k_i+1)(k_i+2)\rho_i^{k_i}}{1-\rho_i^{k_i}}\right) \\ - \left(\frac{\rho_i\left(\frac{1}{1-\rho_i} - (k_i+1)\frac{\rho_i^{k_i}}{1-\rho_i^{k_i+1}}\right)}{\lambda_i\left(1-P(N_i=k_i)\right)}\right)^2. \end{aligned} \tag{15}$$

The approximation of the objective function (Equation (5)) provided by the physical component is a differentiable closed-form expression that depends on three endogenous variables per queue: ρ_i, λ_i and $P(N_i = k_i)$. The Appendix (Section 5) gives the formulation of two auxiliary traffic models used in this paper to approximate Equation (5). That of Section 5.1 is derived in Osorio (2010, Chapter 4) and is used in this paper to address a signal control problem for the Lausanne city-center (Section 3.2). That of Section 5.2 is a formulation that is more efficient for large-scale problems (Osorio and Chong 2015). It is used in this paper to address a signal control problem for the full Lausanne city (Section 3.3).

The use of probabilistic models can lead to differentiable formulations of their non-differentiable deterministic counterparts. For instance, the work in Osorio and Flötteröd (2014) has formulated a probabilistic differentiable formulation of Newell's (deterministic and non-differentiable) simplified theory of kinematic waves (Newell 1993).

In this paper, the queueing network models are not derived from deterministic traditional traffic theoretic models. In particular, they assume a stationary traffic regime, which implies that they do not capture the temporal variations of the probability distributions of network performance. They are simplified models. This simplicity is the key to ensuring the computational efficiency of the underlying SO algorithm. More recently, time-dependent queueing network models that also are sufficiently efficient for simulation-based optimization have been proposed (Chong and Osorio 2017).

2.4. Analytical approximation of $E[T^2]$

We derive the expression for $E[T^2]$, where T denotes the sojourn time at a given queue. We represent an urban road network as a finite capacity queueing network as in Osorio (2010, Chapter 4). Each lane is modeled as one (or a set of) $M/M/1/k$ queue(s). For an $M/M/1/k$ queue the cumulative distribution function $\tilde{F}(t)$ of the sojourn time is given by (cf. Gross et al. (1998), pages 587-641):

$$\tilde{F}(t) = \frac{1-\rho}{1-\rho^k} \sum_{n=0}^{k-1} \rho^n \left(1 - \sum_{m=0}^{n} \frac{(\hat{\mu}t)^m e^{-\hat{\mu}t}}{m!} \right), t \geq 0, \tag{16}$$

with $\hat{\mu}, \rho$ and λ defined in Section 2.3. The probability density function $\tilde{f}(t)$ is obtained as follows:

$$\tilde{f}(t) = \frac{d\tilde{F}(t)}{dt} = -\frac{1-\rho}{1-\rho^k} \sum_{n=0}^{k-1} \rho^n \sum_{m=0}^{n} \frac{\hat{\mu}^m}{m!} \frac{dh(t)}{dt}, \tag{17}$$

where $h(t)$ is defined by:

$$h(t) = t^m e^{-\hat{\mu}t}, t \geq 0. \tag{18}$$

Since:

$$\frac{dh(t)}{dt} = mt^{m-1}e^{-\hat{\mu}t} - \hat{\mu}t^m e^{-\hat{\mu}t}, \tag{19}$$

then:

$$\tilde{f}(t) = \frac{1-\rho}{1-\rho^k} \sum_{n=0}^{k-1} \rho^n \sum_{m=0}^{n} \frac{\hat{\mu}^m}{m!} \left(\hat{\mu}t^m e^{-\hat{\mu}t} - mt^{m-1}e^{-\hat{\mu}t} \right). \tag{20}$$

By definition:

$$E[T^2] = \int_0^\infty t^2 \tilde{f}(t) dt = \int_0^\infty \frac{1-\rho}{1-\rho^k} \sum_{n=0}^{k-1} \rho^n \sum_{m=0}^{n} \frac{\hat{\mu}^m}{m!} \left(\hat{\mu}t^{m+2} e^{-\hat{\mu}t} - mt^{m+1} e^{-\hat{\mu}t} \right) dt. \tag{21}$$

$$E[T^2] = \frac{1-\rho}{1-\rho^k} \sum_{n=0}^{k-1} \rho^n \sum_{m=0}^{n} \frac{\hat{\mu}^m}{m!} \int_0^\infty \left(\hat{\mu}t^{m+2} e^{-\hat{\mu}t} - mt^{m+1} e^{-\hat{\mu}t} \right) dt. \tag{22}$$

According to Gradshteyn and Ryzhik (2007) (pages 247-386):

$$\int_0^\infty t^a e^{-ct^b} dt = \frac{\Gamma(\frac{a+1}{b})}{bc^{(a+1)/b}}, \tag{23}$$

where Γ denotes the gamma function defined as $\Gamma(x) = (x-1)!$.

Using the expression of Equation (23), we obtain the following two equalities:

$$\int_0^\infty \hat{\mu} t^{m+2} e^{-\hat{\mu}t} dt = \hat{\mu} \frac{\Gamma(m+3)}{\hat{\mu}^{m+3}} = \frac{(m+2)!}{\hat{\mu}^{m+2}} \tag{24}$$

$$\int_0^\infty m t^{m+1} e^{-\hat{\mu}t} dt = m \frac{\Gamma(m+2)}{\hat{\mu}^{m+2}} = m \frac{(m+1)!}{\hat{\mu}^{m+2}}. \tag{25}$$

Inserting the expressions of Equations (24) and (25) into (22), leads to:

$$E[T^2] = \frac{1-\rho}{1-\rho^k} \sum_{n=0}^{k-1} \rho^n \sum_{m=0}^{n} \frac{\hat{\mu}^m}{m!} \left(\frac{(m+2)!}{\hat{\mu}^{m+2}} - m \frac{(m+1)!}{\hat{\mu}^{m+2}} \right) \tag{26}$$

$$= \frac{1-\rho}{1-\rho^k} \sum_{n=0}^{k-1} \rho^n \sum_{m=0}^{n} \left(\frac{(m+1)(m+2)}{\hat{\mu}^2} - \frac{m(m+1)}{\hat{\mu}^2} \right) \tag{27}$$

$$= \frac{1-\rho}{1-\rho^k} \sum_{n=0}^{k-1} \rho^n \sum_{m=0}^{n} \frac{2(m+1)}{\hat{\mu}^2} \tag{28}$$

$$= \frac{1-\rho}{1-\rho^k} \sum_{n=0}^{k-1} \rho^n \frac{2}{\hat{\mu}^2} \left(\frac{n(n+1)}{2} + (n+1) \right) \tag{29}$$

$$= \frac{1}{\hat{\mu}^2} \frac{1-\rho}{1-\rho^k} \sum_{n=0}^{k-1} (n+1)(n+2)\rho^n. \tag{30}$$

The above summation can be further simplified, for $\rho \neq 1$, as follows:

$$\sum_{n=0}^{k-1} (n+1)(n+2)\rho^n = \sum_{n=0}^{k-1} \frac{d^2(\rho^{n+2})}{d\rho^2} = \frac{d^2 \left(\sum_{n=0}^{k-1} \rho^{n+2} \right)}{d\rho^2} = \frac{d^2 \left(\rho^2 \frac{1-\rho^k}{1-\rho} \right)}{d\rho^2}. \tag{31}$$

We first calculate the first derivative with regards to ρ:

$$\frac{d \left(\rho^2 \frac{1-\rho^k}{1-\rho} \right)}{d\rho} = \frac{2\rho - (k+2)\rho^{k+1}}{1-\rho} + \frac{\rho^2 - \rho^{k+2}}{(1-\rho)^2}. \tag{32}$$

We then take the first derivative of (32) with regards to ρ:

$$\begin{aligned} \frac{d \left(\frac{2\rho-(k+2)\rho^{k+1}}{1-\rho} + \frac{\rho^2-\rho^{k+2}}{(1-\rho)^2} \right)}{d\rho} &= \frac{2-(k+1)(k+2)\rho^k}{1-\rho} + \frac{2\rho-(k+2)\rho^{k+1}}{(1-\rho)^2} \\ &\quad + \frac{2\rho-(k+2)\rho^{k+1}}{(1-\rho)^2} + \frac{2(1-\rho)(\rho^2-\rho^{k+2})}{(1-\rho)^4} \\ &= \frac{2(\rho^2-\rho^{k+2})}{(1-\rho)^3} + \frac{4\rho-2(k+2)\rho^{k+1}}{(1-\rho)^2} + \frac{2-(k+1)(k+2)\rho^k}{1-\rho}. \end{aligned} \tag{33}$$

Inserting the above expression into (30), we obtain:

$$E[T^2] = \frac{1-\rho}{\hat{\mu}^2(1-\rho^k)}\left(\frac{2(\rho^2-\rho^{k+2})}{(1-\rho)^3}+\frac{4\rho-2(k+2)\rho^{k+1}}{(1-\rho)^2}+\frac{2-(k+1)(k+2)\rho^k}{1-\rho}\right) \quad (34)$$

$$= \frac{1}{\hat{\mu}^2}\left(\frac{2\rho^2}{(1-\rho)^2}+\frac{4\rho}{1-\rho}-\frac{2k\rho^{k+1}}{(1-\rho^k)(1-\rho)}+\frac{2-(k+1)(k+2)\rho^k}{1-\rho^k}\right) \quad (35)$$

$$= \frac{1}{\hat{\mu}^2}\left(\frac{4\rho-2\rho^2}{(1-\rho)^2}-\frac{2k\rho^{k+1}}{(1-\rho^k)(1-\rho)}+\frac{2-(k+1)(k+2)\rho^k}{1-\rho^k}\right). \quad (36)$$

2.5. Methodological summary

Let us summarize the proposed methodology. The considered reliable SO problem is given by Equations (5)-(7). It is addressed with the metamodel SO framework described in Section 2.1. At every iteration of the algorithm, a metamodel optimization problem is solved (Step 3a of Figure 1). The exact formulation of this problem is given by Equations (40)-(46) and is detailed in the Appendix (Section 7).

The key idea of this framework is that the metamodel (defined by Equation (3)) is based upon an analytical approximation of the simulation-based objective function (Equation (5)) derived from an analytical network model. This analytical approximation is represented by the term f_A of Equation (3). The analytical expression of f_A is

$$f_A(x,y;q) = E[\sum_{i\in\mathscr{Q}} T_i(x,y;q)] + r\sqrt{\sum_{i\in\mathscr{Q}} Var[T_i(x,y;q)]}, \quad (37)$$

where $E[\sum_{i\in\mathscr{Q}} T_i(x,y;q)]$ is given by Equations (8), (9) and (10), $Var[T_i(x,y;q)]$ is given by Equation (15) and $\mathscr{Q}$ represents the set of queues (or lanes) in the network. The analytical network models used to derive f_A in the two case studies of this paper are formulated in the Appendix (Sections 5.1 and 5.2).

At every iteration of the SO algorithm, the metamodel combines information from the simulation-based network model with information from the analytical network model. More specifically, at every iteration, the parameters of the metamodel (α and β of Equation (3)) are fitted such as to minimize a distance metric between the simulation observations and the metamodel approximations at the set of sample points.

3. Case studies

3.1. General description

We evaluate the performance of this framework based on a calibrated microscopic traffic simulation model of the Lausanne city center developed by Dumont and Bert (2006). It is calibrated for the Lausanne city road network during evening peak period (17h-18h). It is implemented in Aimsun (TSS 2011). For a more detailed description of the network and the demand, see Osorio (2010,

	Traffic model	
	Simulation-based microscopic	Analytical macroscopic
Metamodel m	$\surd$	$\surd$
Metamodel ϕ	$\surd$	

Table 1 Comparison of different metamodel approaches.

Chapter 4). We address signal control problems within two networks: (i) the Lausanne city center (Section 3.2), (ii) the full city network (Section 3.3).

We compare the performance of the following SO metamodel approaches:

- the proposed metamodel, m (of Equation (3));
- a quadratic polynomial with diagonal second-derivative matrix, (i.e. the metamodel consists of ϕ as defined in Equation (3)). In this approach, the metamodel consists of only a functional component, there is no physical component.

A comparison of these two approaches is presented in Table 1. This table indicates that the proposed metamodel m combines information from both the simulation-based microscopic model and from the analytical macroscopic model (the queueing network model), whereas the metamodel ϕ uses only information obtained from the microscopic simulator. Hence, the comparison of methods m and ϕ indicates the added value of coupling the microscopic simulated information with macroscopic analytical information.

We evaluate the performance of both metamodel methods by addressing three different signal control problems that vary according to their objective function.

- P1: this is a traditional signal control problem which uses only first-order moment information (i.e., travel time expectation information) in the objective function, which is given by $E[\sum_{\mathscr{L}} T_i(x,z;p)]$.
- P2: this is the reliable signal control problem, with the objective function given by Equation (5).
- P3: this signal control problem uses only standard deviation information in the objective function, which is given by $SD[\sum_{\mathscr{L}} T_i(x,z;p)]$.

Problem P2 requires the estimation of the reliability ratio parameter r. Recall that the mean-variance approach considers functions of the form $t_E + rt_V$, where t_E denotes the expected trip travel time and t_V denotes the standard deviation of trip travel time. In order to identify a suitable r value, we reviewed travel time and travel time variability valuation studies. The estimates for r vary according to, for instance, the network, the time-of-day and the trip purpose. In past work, where t_V is defined as the standard deviation of trip travel time, estimates of r have varied between 0.1 (Hollander 2006) and 2.1 (Batley and Ibáñez 2009). Black and Towriss (1997) estimate an r value of 0.79 for commuters traveling with a car. More recently, Li, Hensher and Rose (2010) derived a value of 1.43 for car commuters.

We consider evening peak period traffic, where most trips consist of commuters. Additionally, the simulation model that we use represents only car traffic. Thus, we use the value of 1.43, which was estimated for car commuters by Li, Hensher and Rose (2010). Additionally, the largest r value found in the literature (value of 2.1) is used to evaluate the sensitivity of our approach to r (Section 3.4).

Note that the r estimates derived from these surveys are obtained by using trip travel time as the travel time metric, whereas in this paper we use total link travel time. Thus, the actual r value derived from an analysis that would consider total link travel time for the evening peak period of Lausanne, may differ from the value of 1.43 that we use.

For all experiments the computational budget is set to 150 runs, i.e., a signal plan with improved performance needs to be identified within 150 simulation runs. Given the stochasticity of the simulation outputs as well as the large-scale problems that we are addressing, these are considered very tight computational budgets. For a description of how the simulation runs are allocated across iterations see Appendix (Section 6) and also Osorio and Bierlaire (2013).

When evaluating the performance of a given method, we need to account for the fact that the outputs of the simulator are stochastic. For a given experiment (i.e., a given combination of: metamodel, objective function, network, initial point and computational budget) we run the SO algorithm five times. Each algorithmic run yields a proposed signal plan. Thus a given experiment yields 5 signal plans. We then compare the performance of these proposed signal plans across experiments.

In order to evaluate the performance of a proposed signal plan, 50 simulation replications are run. This yields 50 observations of the expected total link travel time and total link travel time standard deviation. We then plot the empirical cumulative distribution function (cdf) of each of these 2 performance metrics, and compare the cdf's obtained by different methods.

3.2. Lausanne city center

The Lausanne city network is represented in Figure 2. The city center of interest is delimited by an oval. It contains 48 roads and 15 intersections, 9 of which are signalized and control the traffic on 30 roads.

A total of 51 signal phases are endogenous. The queueing model of this network consists of 102 queues. The trust region subproblem that is solved at each iteration of the SO algorithm (which is defined in the Appendix by Equations (40)-(46)) consists of 621 endogenous variables with their corresponding lower bound constraints, 408 nonlinear equality constraints and 171 linear equality constraints.

Figure 3 displays six plots. The plots in a given column correspond to a given initial point. The plots of a row correspond to a given performance measure. The upper (resp. lower) row displays

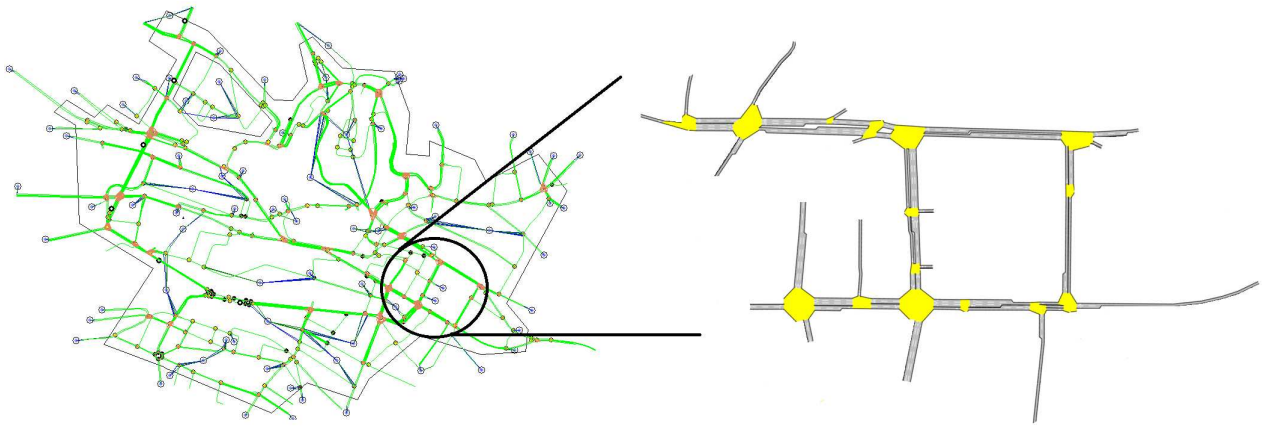

Figure 2 **Lausanne city network model with city center delimited by a circle (left), city center of interest (right).**

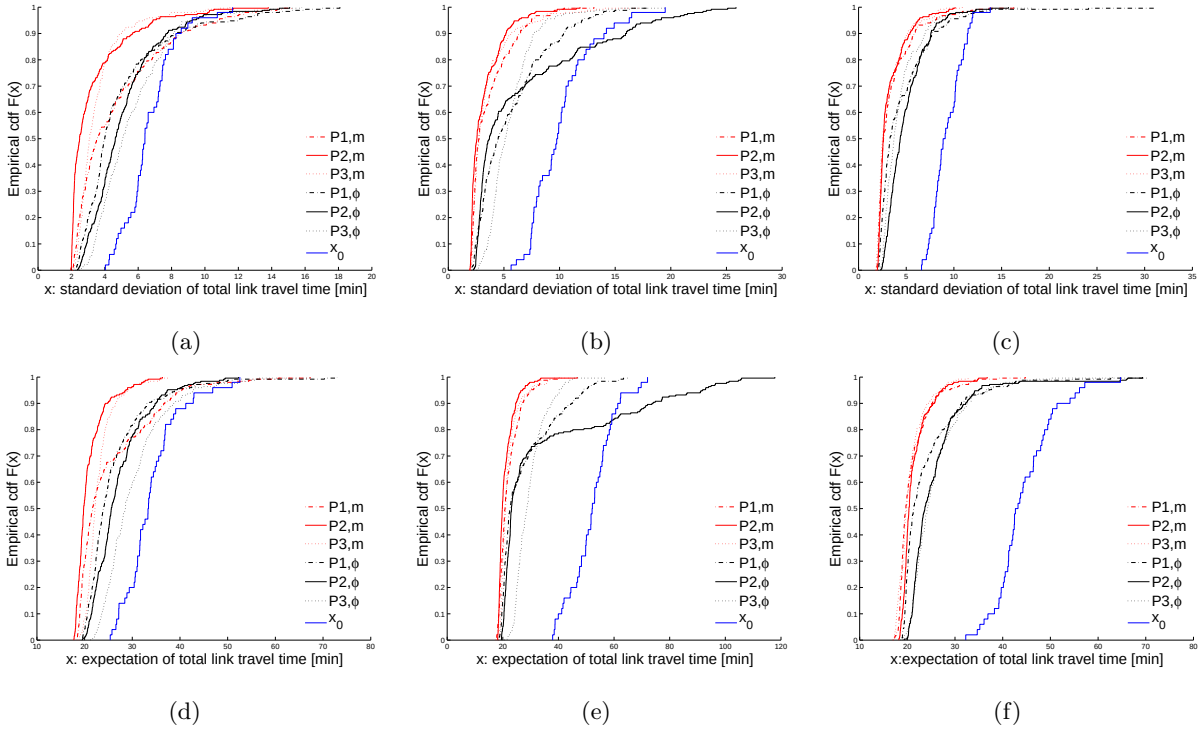

Figure 3 **Performance of the signal control methods when applied to the Lausanne city center. These plots consider various initial points and various problem formulations.**

the cdf's of the standard deviation (resp. expectation) of total link travel time (within the city center). Each plot displays 7 cdf's: the solid blue cdf corresponds to the cdf of the initial signal plan (denoted x_0), the remaining 6 cdf's correspond to solving a given problem (P1, P2 or P3) with a given metamodel method (m or ϕ). The red (resp. black) cdf's correspond to the signal plans obtained when using m (resp. ϕ). The initial points are uniformly drawn from the feasible space (Equations (6) and (7)) using the code of Stafford (2006).

Recall that when solving a given problem with a given metamodel, we run the SO algorithm 5 times, yielding 5 signal plans, and then evaluate each of the 5 proposed signal plans by running 50 simulation replications. The cdf's displayed in Figure 3 are obtained by aggregating (for a given problem and a given metamodel) the observations from all 5 signal plans, i.e. they consist of 5*50 observations.

For the first initial point (column 1), the signal plans with best performance both in terms of expectation and standard deviation are obtained by solving P2 (i.e., a problem that combines expectation and standard deviation information) and using the proposed metamodel, m. The signal plans derived by using m outperform those derived by the traditional metamodel ϕ regardless of the problem formulation (i.e., for all P1, P2 and P3). Similar conclusions hold for both the second initial point (column 2) and the third initial point (column 3).

All plots of Figure 3 indicate that using metamodel m to solve problem P2 leads to signals plans with both: (i) the lowest average standard deviation (i.e., highest travel time reliability), as well as (ii) the lowest variance across simulation replications (i.e., the signal plans are robust to the stochasticity of the simulator, in other words they are robust to the uncertainty represented by the simulator). Both contribute to a more reliable and predictable system performance.

Figure 3 also indicates that when using ϕ, the best signal plans are obtained when using only expected total travel time (P1), and the performance deteriorates when higher-order information is included (P2 and P3). This illustrates: 1) the inability of a general-purpose metamodel (in this case a quadratic polynomial) to approximate, in the entire feasible region, intricate objectives functions, such as those that account for higher-order distributional information, as well as 2) the added value of using auxiliary traffic models (in this case a queueing network model) to solve such problems.

When comparing the use of ϕ to address the formulation that includes only standard deviation (P3) with the formulation that includes both expectation and standard deviation (P2), the latter leads to standard deviations that are either similar or better, which is counterintuitive. This may be explained as follows. Firstly, formulation P1 (only expectation information) leads to low standard deviation values, thus the expectation and standard deviation metrics may be positively correlated. Second, the expectation metric has less variability across simulation replications, thus it can be estimated more accurately with few simulation replications, leading to a better algorithmic performance for tight computational budgets. For these 2 reasons,the formulations that include expectation information (P1 and P2) lead to improved standard deviation, and particularly when considering tight computational budgets.

Figure 4(a) considers all 3 initial points and all solutions obtained from addressing problem P2 with methods m and ϕ of Figure 3. Figure 4(a) displays 9 cdf's of the simulation-based objective function (Equation (5)). Since we consider a minimization problem, the more a cdf curve is shifted

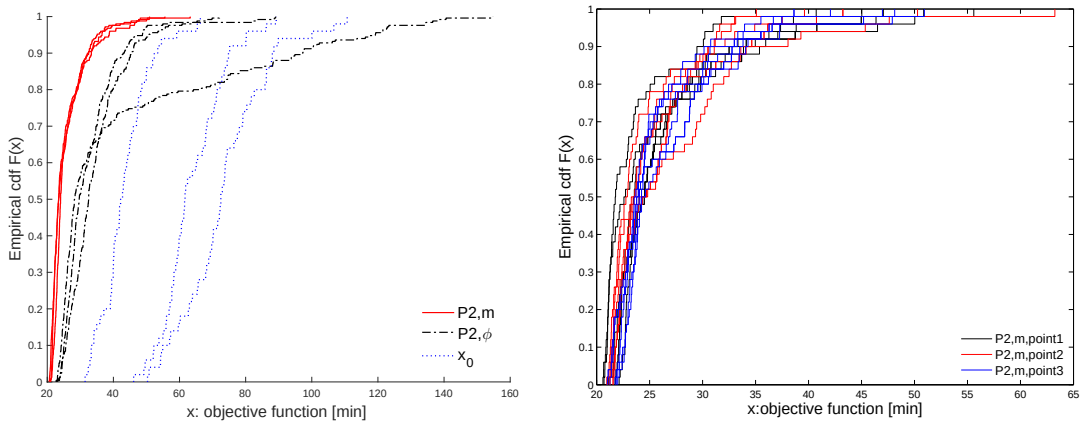

(a) (b)

Figure 4 Performance of the methods when applied to problem P2 with 3 different initial points.

to the left, the better the performance of the corresponding method. The 3 blue dotted cdf's correspond to the 3 initial points. The three red solid (resp. black dashed) cdf's correspond to method m (resp. ϕ). Each of the red and black cdf curves corresponds to the solutions obtained with a given initial point. Just as for Figure 3, each of these curves aggregates the observations from all 5 solutions derived by the 5 SO runs of the algorithm.

Figure 4(a) shows that the solutions of method m outperform those of method ϕ, and this for all initial points. In other words, the aggregate performance of the 15 solutions proposed by method m outperforms the 15 solutions of method ϕ. Figure 4(a) shows that the different initial points have very different performance (i.e., the three blue dotted curves have very different performance). Nonetheless, all three curves of method m have very similar performance. This indicates that the solutions of method m are not sensitive to the quality of the initial points. For method ϕ, one of its three curves has very different performance compared to the other two. Hence, the solutions of method ϕ are sensitive to the initial points. Additionally, the three curves of method m have similar variability. This indicates that the solutions of the method are not sensitive to the stochasticity of the simulator. For method ϕ, the cdf curves have a higher variability, i.e., there is a higher variance in the performance of the method for a given initial point. This indicates that method ϕ is more sensitive than method m to the simulator's stochasticity. Figure 4(a) also indicates that for method ϕ the magnitude of the variance depends on the inital point. Recall that methods m and ϕ only differ in whether or not they use information from the analytical macroscopic model. Hence, this figure illustrates that by providing the algorithm with this analytical information, we improve the robustness of the SO algorithm to both: (i) initial points, and (ii) simulator stochasticity.

Figure 4(b) presents in more detail the performance of method m for different initial points. It displays the 15 cdf's of the 15 solutions obtained when solving problem P2. While Figure 4(a)

displayed one cdf per initial point (i.e., the cdf aggregated the performance of all 5 solutions), this figure displays one cdf per initial point and per solution. The cdf's that correspond to solutions obtained with the same initial point have the same color. This figure shows that all cdf's are similar regardless of their color. This means that the solutions are robust to the quality of the initial point.

The cdf's presented so far display the performance aggregated across all links of the city center. Figure 5 illustrates the performance at the link level. This figure displays two plots of the city center network. The links of the network are color coded according to their link travel time standard deviation. The colors green, yellow and red correspond, respectively, standard deviations that are lower than 20 seconds, are between 20 and 40 seconds, and are greater than 40 seconds. These standard deviation estimates are obtained by running 50 replications of a given signal plan. The top network considers the initial plan (that of column 1 of Figure 3), the bottom network considers one of the plans proposed by using that initial plan and the metamodel m to solve the reliable signal control problem P2. Figure 5 shows that there is an improvement across the entire city center. This illustrates that the proposed approach leads to both improvements when aggregating across links (e.g., total link travel time), as well as systematic improvements at the link level.

3.3. Lausanne city

In this section, we address a signal control problem that controls intersections across the entire city of Lausanne. Figure 6 displays the road network of the city, Figure 7 displays the corresponding network model. The full network contains 603 roads and 231 intersections, we determine the plans for 17 intersections, which are represented as filled rectangles in Figure 7.

A total of 99 signal phases are endogenous. The queueing model consists of 902 queues. The trust region subproblem that is solved at each iteration of the SO algorithm (which is defined in the Appendix by Equations (40)-(46)) consists of 2805 endogenous variables with 1821 nonlinear equality constraints and 902 linear equality constraints. The problem we address in this section is considered a large-scale traffic signal control problem and a difficult high-dimensional simulation-based optimization problem.

In order to compare the performance of the methods across various problems, we proceed as for the city center (i.e., Section 3.2). Figure 8 displays six plots: each column corresponds to a given initial point, each row corresponds to a given performance measure. The upper (resp. lower) row displays the cdf's of the standard deviation (resp. expectation) of total link travel time within the full city network. Each cdf aggregates 250 (i.e., 5*50) simulation observations.

For the first initial point (column 1), the signal plans with best performance both in terms of expectation and standard deviation are obtained by solving P2 (i.e., a problem that combines expectation and standard deviation information) and using the proposed metamodel, m. The signal

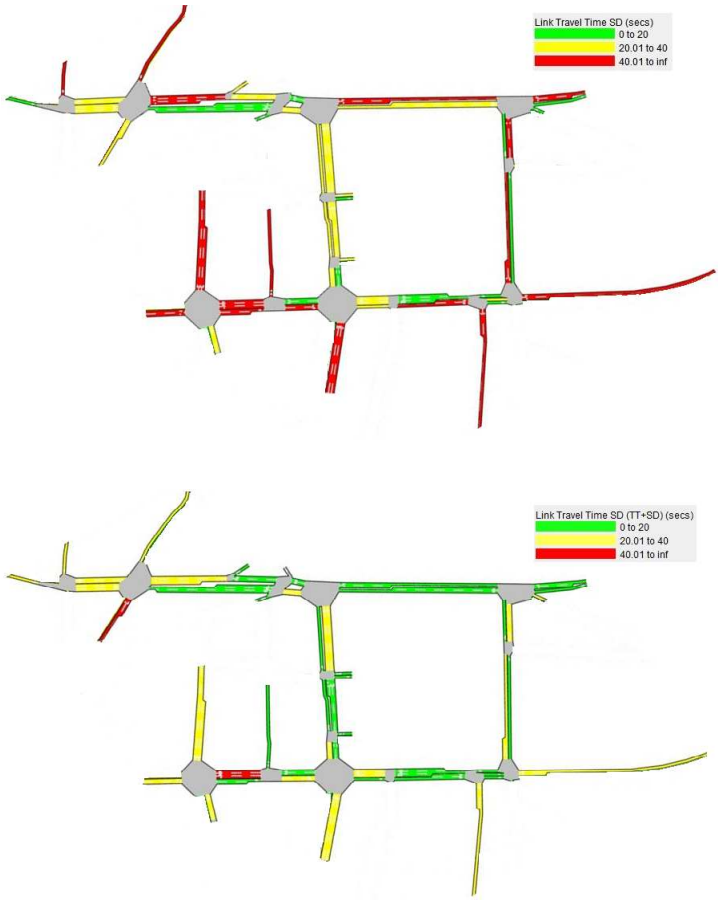

Figure 5 **Link based travel time standard deviation for initial plan (top plot) and plan obtained by solving problem P2 with metamodel m (standard deviation estimates are obtained by averaging over 50 replications).**

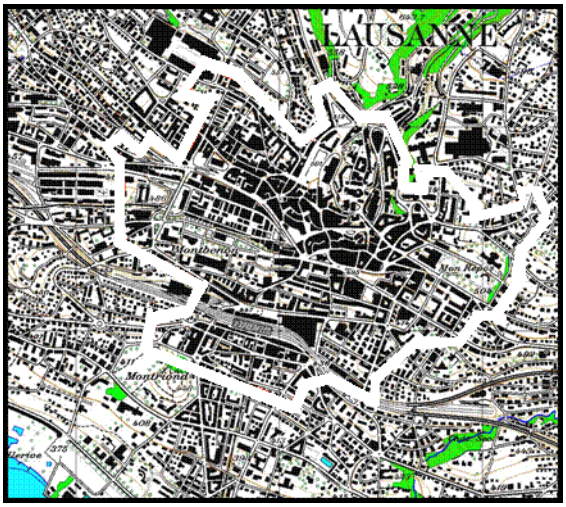

Figure 6 **Lausanne city road network (adapted from Dumont and Bert (2006)).**

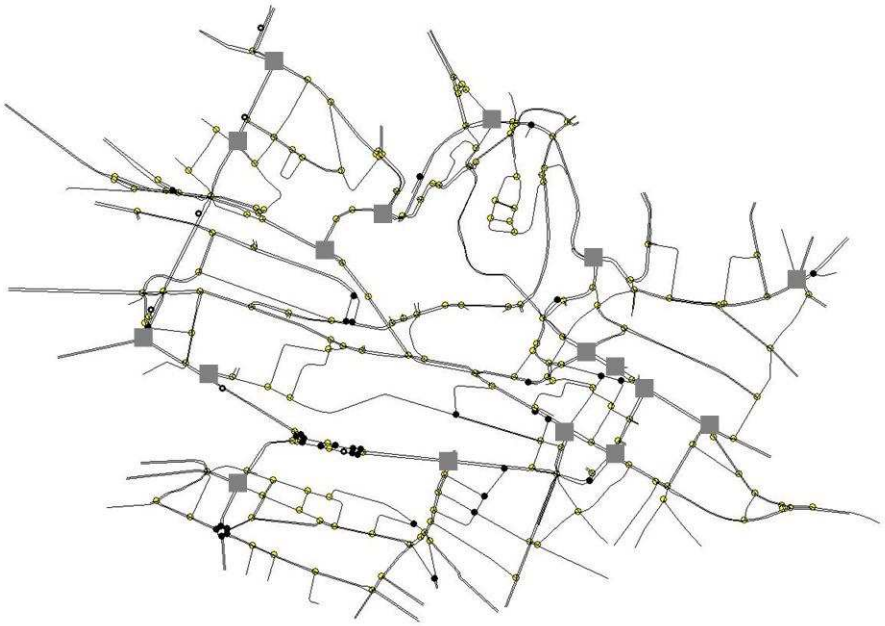

Figure 7 **Lausanne network model with the 17 controlled intersections displayed as grey rectangles.**

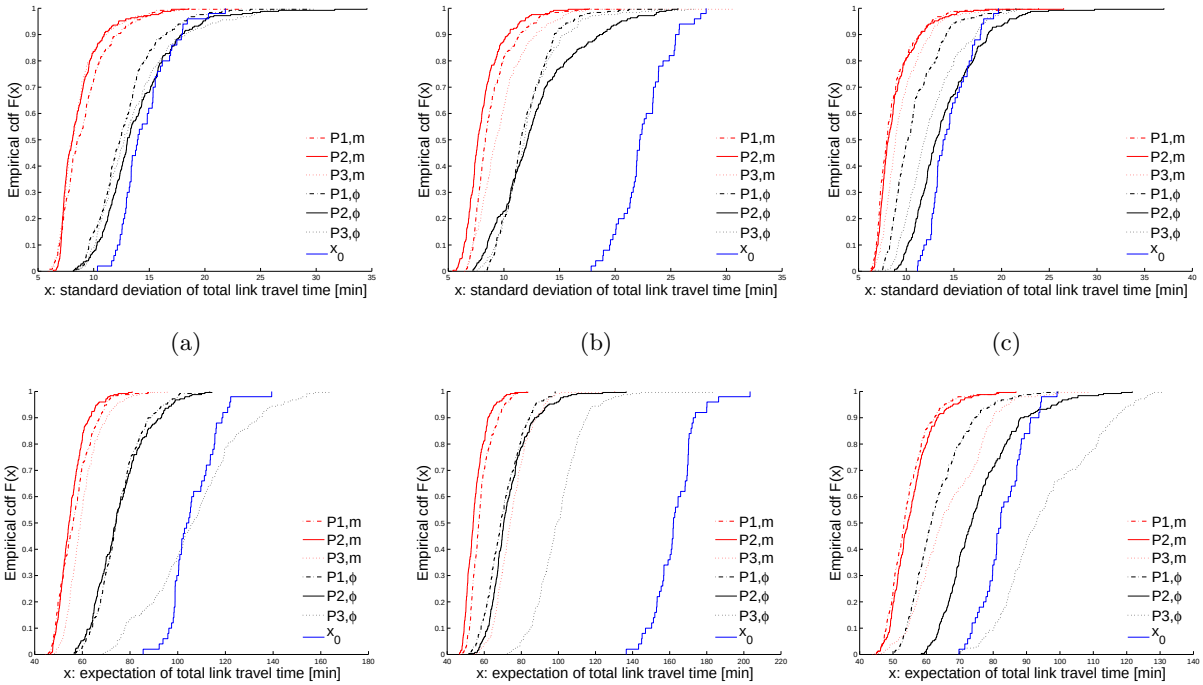

Figure 8 **Performance of the signal control methods when applied to the full city of Lausanne. These plots consider various initial points and various problem formulations.**

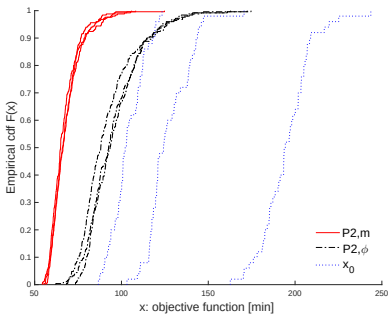

Figure 9 Performance of the methods when applied to the full city problem P2 with 3 different initial points.

plans derived by using m and solving any of the three problems outperform those derived by the traditional metamodel ϕ. Similar conclusions hold for initial points 2 (column 2) and 3 (column 3).

The plans obtained by using only standard deviation information (i.e. solving P3) with metamodel m still provide improvement in terms of expected travel time (see row-wise plots) when compared to the initial point, whereas those derived by ϕ fail to do so for initial points 1 and 3.

As for the city center case study, the plots of Figure 8 indicate that using metamodel m to solve problem P2 leads to signals plans with low average and variance of the standard deviation. Both indicators enhance the travel time reliability of the network.

We proceed just as for the city center case study and analyse the sensitivity of the SO algorithms to the quality of the initial points and to the simulator's stochasticity. Figure 9 considers all 3 initial points and all solutions obtained from addressing problem P2 with methods m and ϕ of Figure 8. Figure 9 displays 9 cdf's of the simulation-based objective function (Equation (5)): the 3 blue dotted cdf's correspond to the 3 initial points, the 3 red solid (resp. black dashed) cdf's correspond to method m (resp. ϕ). Just as for the city center case study, Figure 9 shows that the solutions of method m outperform those of method ϕ, and this for all initial points. In other words, the aggregate performance of the 15 solutions of method m is better than that of the 15 solutions of method ϕ. Figure 9 shows that the different initial points have very different performance, while all three curves of method m are very similar. The curves of method ϕ are also similar, yet less so than for method m. This indicates that both methods are robust to the quality of the initial solution. Also for both methods, their 3 curves have similar variability. The variability of the curves of method m is smaller than those of method ϕ.

We now compare the performance of methods m and ϕ with different computational budgets. We proceed as in Figure 9, i.e., we consider problem P2 and all three initial points. Figure 10 displays 12 plots. The plots in a given column correspond to a given computational budget. Columns 1, 2, 3, and 4, respectively, consider budgets of 20, 50, 100, and 150 simulation runs.

Let us first present and analyse the plots in the first 2 rows. The plots in the first (resp. second) row consider method ϕ (resp. m). Each plot displays 18 cdf's: the 3 dotted blue cdf's correspond

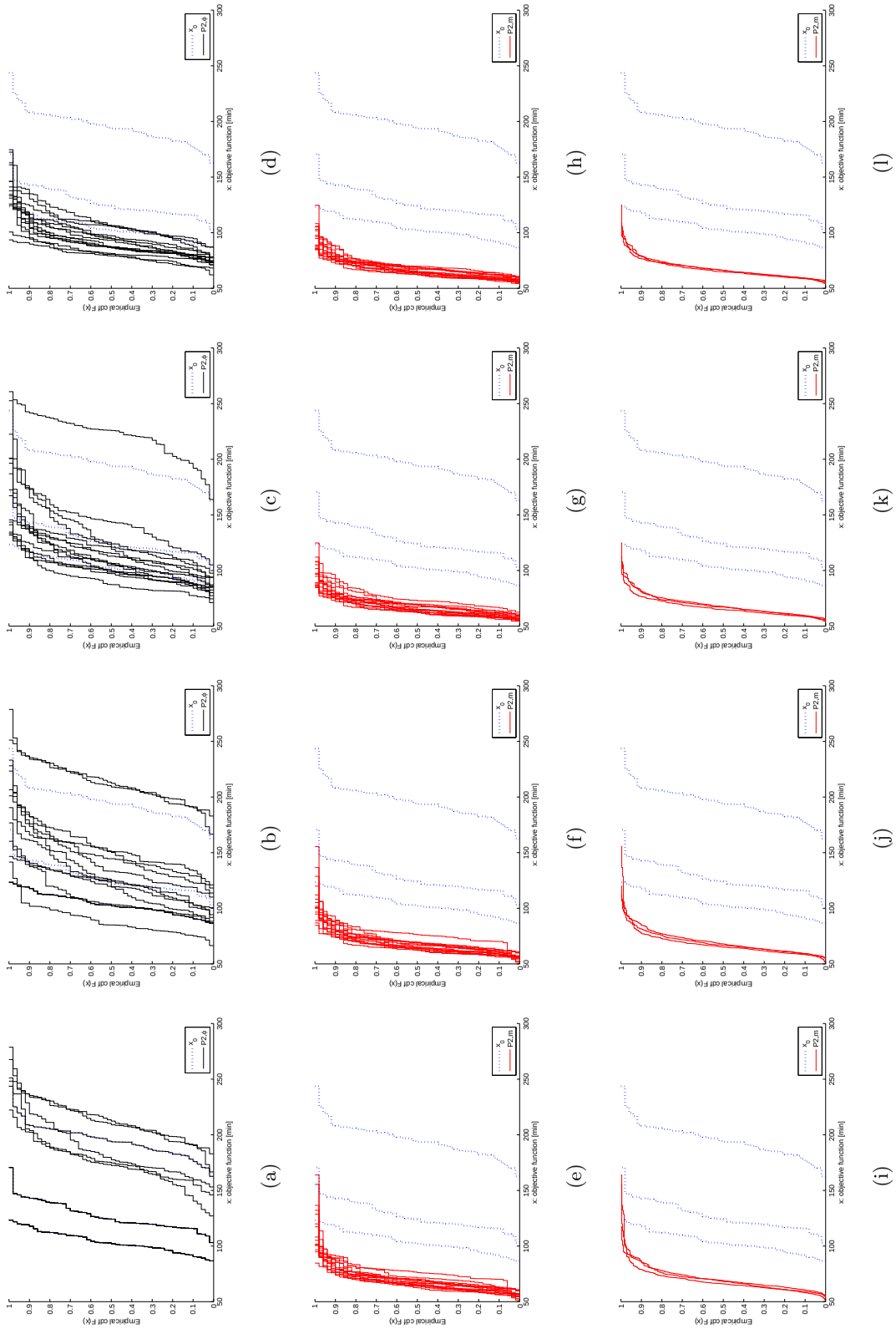

Figure 10 **Performance of the methods when applied to the full city problem P2 with 4 different computational budgets.**

to the 3 different initial signal plans (denoted x_0), the remaining 15 cdf's correspond to solving problem P2 with a given metamodel method (m or ϕ) 5 times for each initial point (for a total of 5*3=15 times). The black (resp. red) cdf's correspond to solutions derived by ϕ (resp. m). All plots have the same x-axis limits, i.e., they can be directly compared. The first row of plots indicates that as the computational budget increases, so does the performance of the solutions proposed by ϕ. For small budgets (e.g., 20 or 50) the signal plans proposed by ϕ tend to have similar or worse, performance compared to the initial points. For larger budgets (e.g., 100 or 150), their performance is similar or slightly better than that of the best initial point. The second row of plots indicates that the signal plans proposed by m have consistently good performance even for very small budgets. In other words, for all budgets (20, 50, 100 or 150), the method m identifies signal plans with good performance. Additionally, for a given budget (i.e., a given plot in the second row) the performance of the 15 plans proposed by m have similar performance. This indicates the robustness of the method to both the quality of the initial point, as well as to the stochasticity of the simulator.

The third row of plots considers the performance of P2 across both computational budgets and initial points. Each plot displays 6 cdf's: 3 dotted blue cdf's that correspond to the initial points and 3 red cdf's that correspond to the aggregate performance of method m for a given initial point. In other words, each red cdf considers a given initial point and aggregates the performance of all 5 SO runs (hence each red curve consists of 5*50 simulation observations). For each budget, the 3 red cdf's are very similar. This indicates that, for a given computational budget, the performance of method m is robust to the initial point. This holds true for all four plots of the third row, i.e., for all computational budgets, method m is robust to the quality of the initial point.

Figure 11 displays the link-level results for a part of the city network. Each plot displays the link standard deviation (averaged over 50 simulation replications). The top plot considers initial point 2, and the bottom plot considers a signal plan proposed by solving P2 and using the metamodel m, given initial point 2. The colors green, yellow and red correspond, respectively, to values smaller than 20 seconds, from 20 to 40 seconds, and greater than 40 seconds. Just as for the city center, there is a systematic improvement at the link level. This shows that the proposed plan reduces both the total variability as well as the individual link travel time variability.

3.4. Sensitivity to reliability ratio

In this section, we evaluate the sensitivity of our proposed approach to the value of the reliability ratio parameter r. We choose the highest r value found in the literature, namely 2.1. We address the reliable signal control problem P2 with the proposed metamodel m. We compare the performance of an approach that sets r to 1.43 to one that sets r to 2.1. The sensitivity analysis serves the purpose of illustrating that the proposed methodology performs well for various values of r.

Figure 11 **Link travel time standard deviation for initial plan (top plot) and plan obtained by solving problem P2 with metamodel m (standard deviation estimates are obtained by averaging over 50 replications).**

We proceed as in Sections 3.2 and 3.3: we consider an initial point, and run each approach 5 times, deriving 5 signal plans. We then evaluate the performance of each of these signal plans by running 50 simulation replications.

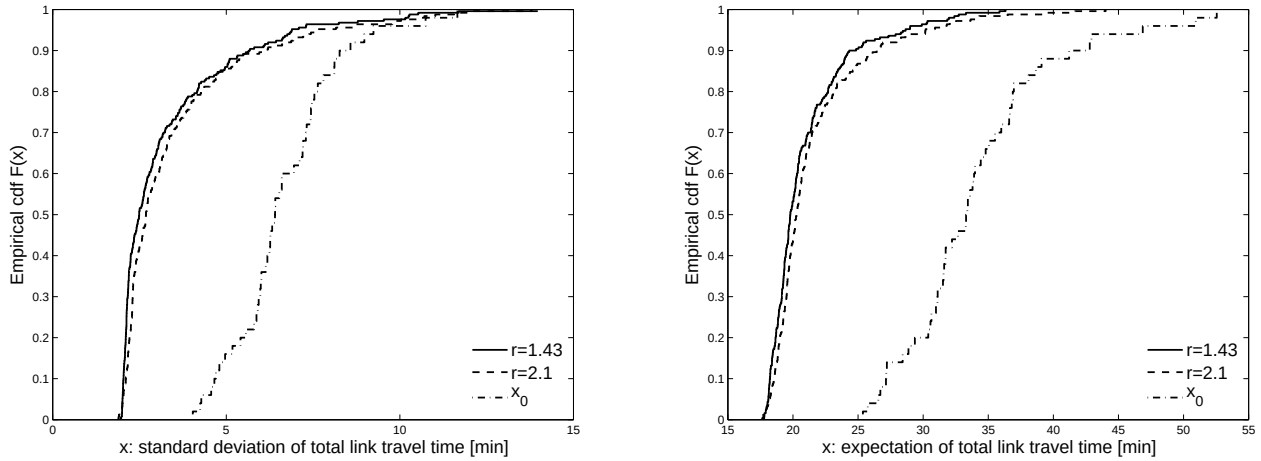

Figure 12 **Empirical cdf's of the total link travel time standard deviation (left plot) and expected total link travel time (right plot) with different reliability ratio values.**

Figure 12 displays two plots. The left (resp. right) plot displays the cdf's of the standard deviation (resp. expectation) of total link travel time. Each cdf consists of 5*50 simulation observations (i.e., 5 signal plans with 50 simulation replications for each signal plan). The cdf of the initial signal plan corresponds to the dash-dotted curve, the cdf for the signal plans derived with $r = 1.43$ (resp. $r = 2.1$) is the solid (resp. dashed) curve. Solving the problem P2 with these two different reliability ratio values leads to signal plans with similar performance. The methodology seems insensitive to such changes in the reliability ratio values. Recent research has indicated a positive correlation between the expectation and the standard deviation of travel time metrics (Mahmassani et al. 2012, 2013). This may contribute to the insensitivity of the approach to the value of the reliability ratio.

3.5. Computational Efficiency

Each iteration of the SO algorithm involves two computational intensive tasks: 1) running the simulator; 2) solving the trust region subproblem (defined by Equations (40)-(46)). In this section, we compare the run time needed for each of these tasks. We solve the subproblem with the Matlab (Mathworks, Inc. 2011) *fmincon* routine for constrained nonlinear problems, and use its sequential quadratic programming algorithm (Coleman and Li 1996, 1994). Details on how the subproblem is solved are given in Osorio and Bierlaire (2013).

For a given initial point, we solve problem P2 five times allowing each time for 150 SO iterations. The computer used for calculation has a processor of Intel Core i7, 3.50 Ghz and RAM of 8GB. Figure 13 displays the cdf of all 5*150 computational run time observations. The left (resp. right) plot displays the run times for the Lausanne city center (resp. full Lausanne city). The solid cdf curve displays the run time needed for the convergence of the trust region subproblem, whereas the

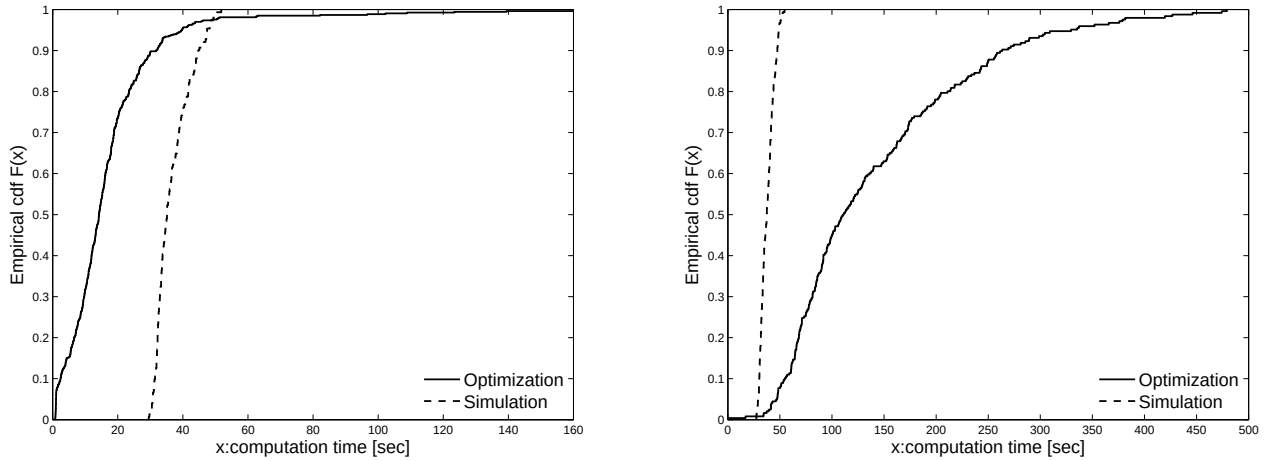

Figure 13 Computational run time for Lausanne city center (left) and full Lausanne city (right).

dashed cdf curve displays the run time for one simulation replication. The simulation run time is relatively constant across iterations, with run times of the order of 30 seconds, and not exceeding 60 seconds. The trust region subproblem is solved quicker than a single simulation run in the city center case study. For the full city case study, it can be of the order of several minutes (i.e., several simulation replications). This illustrates the computational efficiency of the overall SO framework.

4. Conclusion

This paper presents a method to address a reliable signal control problem by using higher-order distributional information derived from a stochastic simulator. The objective function is a linear combination of the expectation and the standard deviation of total link travel time. Distributional travel time estimates are derived from a detailed stochastic microscopic urban traffic simulator. They are combined with analytical approximations, which are obtained from differentiable probabilistic macroscopic traffic models. A metamodel simulation-based optimization (SO) algorithm is used.

The proposed SO approach is compared to a traditional SO approach. Three different signal control formulations are considered. Experiments on the Lausanne city center network and the full city network are carried out. The SO methods are evaluated within tight computational budgets, where the simulator can only be evaluated a total of 150 times. The proposed SO approach outperforms the traditional approach, in particular for formulations including the standard deviation of link travel time. The use of the proposed method to solve a reliable signal control problem leads to signal plans with the lowest expected total link travel time and the lowest standard deviation of total link travel time. These signal plans also have the lowest variability across simulation replications of the travel time standard deviation. The proposed approach systematically outperforms the

traditional approach. It leads to aggregate improvements (total link metrics), as well as link-level improvements.

The proposed method enables the use of highly detailed distributional information provided by these stochastic simulators to inform the design and operations of urban transportation networks. Such an approach can be used to efficiently address other reliable and robust formulations of traditional transportation problems. Of ongoing interest is also the development of traffic-responsive reliable traffic management strategies. We have recently proposed a tractable traffic-responsive SO algorithm (Chen et al. 2015). Such ideas could be combined with the ideas presented in this paper to develop traffic-responsive reliable strategies.

As high-resolution urban mobility data (e.g., smart-phone data, vehicle trajectory data) becomes more readily available, it opens the way for more intricate optimization problems to be addressed (e.g., network reliability , network robustness). To enable the use of detailed traffic models to address such problems will require proper calibration and validation of these novel performance metrics (e.g., reliability metrics, robustness metrics). This opens the way for a variety of novel and challenging calibration problems that aim to fit higher-order distributional metrics. Metamodels can play an important role in this area. For instance, as part of ongoing work we are exploring the use of the analytical travel time expressions derived in this paper to design calibration algorithms that fit both first- and second-order moments of the data (e.g., travel time, flows).

In this paper, we considered green splits as the decision vector. The proposed framework can be used to address other types of problems with continuous decision variables. First, *any* continuous variable can be included in the polynomial term of the metamodel (ϕ in Equations (3) and (4)). In other words, the framework can be directly applied to the optimization of any continuous simulation-based optimization problem. Second, a computationally efficient formulation can be obtained by including the decision variable both in the polynomial term and in the physical component term (f_A in Equation (3)). The latter can be achieved by using a macroscopic model formulation that explicity depends on all decision variables. For instance, in Equation (43) (of the Appendix Section 7), the cycle times, c, are related to the flow capacities of the controlled lanes, μ, and to the green splits, x. The current formulation can therefore be directly used for cycle time optimization. For offset optimization, we would recommend the use of a time-dependent macroscopic model. We have recently formulated a tractable and scalable time-dependent analytical network model that has been used succesfully for dynamic simulation-based optimization (Chong and Osorio 2017). It is being used, as part of an ongoing collaboration with a regional transportation agency to study offset optimization problems. On the other hand, stage structure optimization is typically formulated as a discrete optimization problem. This requires the formulation of a (non-convex and constrained) simulation-based optimization algorithm for mixed-integer problems. We are unaware of computationally efficient algorithms for such problems.

Every iteration of the proposed SO algorithm, evaluates the performance of a set of points (i.e., signal plans) with two types of traffic models: (i) a stochastic dynamic microscopic traffic model (simulation-based model), (ii) a probabilistic stationary analytical macroscopic traffic model. The purpose of the analytical model is to enhance the computational efficiency of the algorithm. It should therefore be a highly efficient model. In this paper, the microscopic simulator considers dynamic and endogenous traffic assignement (i.e., the assignement depends on time-varying congestion levels and on network supply conditions such as signal plans), while the macroscopic analytical model considers time-independent and exogenous traffic assignement. One extension of this work is to use a macroscopic model with time-dependent and endogenous assignement. Computationally efficient analytical formulations with endogenous assignement suitable for SO and for large-scale networks have been recently proposed for both traffic management problems (Osorio and Selvam 2017), as well as for calibration problems for the Berlin metropolitan area (Zhang et al. 2017). The extension of such formulations for reliable SO problems is of interest. As discussed in Section 2.1, the proposed framework can be used with any macroscopic model that is scalable and efficient. Ongoing work studies the use of traditional traffic flow theoretic network models for SO.

The simulation-based traffic model accounts in detail for the between-link dependencies, while the auxiliary analytical traffic model has a high-level description of these dependencies. We have recently formulated an analytical technique that is both based on traditional traffic flow theory and that accounts in more detail for the between-link interactions: it derives the joint queue-length distribution of adjacent links (Flötteröd and Osorio 2017). This can enable a more accurate approximation of the link travel time distributions. Ongoing work formulates more tractable formulations of this novel network model, such as to enable its use as an auxiliary traffic model for SO.

Acknowledgements

The work of Xiao Chen is supported by the Portuguese Foundation for Science and Technology (FCT) through grant SFRH/BD/51296/2010. The work of Carolina Osorio is partially supported by the U.S. National Science Foundation under Grant No. 1351512. Any opinions, findings, and conclusions or recommendations expressed in this material are those of the authors and do not necessarily reflect the views of the U.S. National Science Foundation. The authors also thank Dr. Emmanuel Bert and Prof. André-Gilles Dumont (LAVOC, EPFL) for providing the Lausanne simulation model.

Appendix

5. Physical components

5.1. Physical component used in Section 3.2

Recall from Section 2.3 that the analytical approximation of the objective function (Equation (5)) provided by the physical component is a function of three endogenous variables per queue: ρ_i, λ_i and

$P(N_i = k_i)$. We present below the analytical traffic model that derives these variables. This model is based on the general queueing network model of Osorio and Bierlaire (2009). Its formulation for an urban traffic network is given in Osorio (2010, Chapter 4). Each lane of an urban road network is modeled as one or a set of finite capacity queues. The model describes the between-link interactions (e.g., spillbacks) through the queueing theory notion of blocking. It provides an analytical description of how congestion arises and propagates through the network. In the following notation the index i refers to a given queue.

γ_i	external arrival rate;
λ_i	arrival rate (also referred to as total arrival rate);
μ_i	service rate;
$\tilde{\mu}_i$	unblocking rate;
$\hat{\mu}_i$	effective service rate (accounts for both service and eventual blocking);
ρ_i	traffic intensity;
P_i^f	probability of being blocked at queue i;
k_i	upper bound of the queue length;
N_i	total number of vehicles in queue i;
$P(N_i = k_i)$	probability of queue i being full, also known as the blocking or spillback probability;
p_{ij}	transition probability from queue i to queue j;
$\mathscr{D}_i$	set of downstream queues of queue i;

The queueing network model is defined through the following system of nonlinear equations:

$$\begin{cases} \lambda_i = \gamma_i + \dfrac{\sum_j p_{ji}\lambda_j(1 - P(N_j = k_j))}{(1 - P(N_i = k_i))} & \text{(38a)} \\ \dfrac{1}{\tilde{\mu}_i} = \displaystyle\sum_{j \in \mathscr{D}_i} \dfrac{\lambda_j(1 - P(N_j = k_j))}{\lambda_i(1 - P(N_i = k_i))\hat{\mu}_j} & \text{(38b)} \\ \dfrac{1}{\hat{\mu}_i} = \dfrac{1}{\mu_i} + P_i^f \dfrac{1}{\tilde{\mu}_i} & \text{(38c)} \\ P(N_i = k_i) = \dfrac{1 - \rho_i}{1 - \rho_i^{k_i+1}} \rho_i^{k_i} & \text{(38d)} \\ P_i^f = \displaystyle\sum_j p_{ij} P(N_j = k_j) & \text{(38e)} \\ \rho_i = \dfrac{\lambda_i}{\hat{\mu}_i}. & \text{(38f)} \end{cases}$$

The exogenous parameters are γ_i, μ_i, p_{ij} and k_i. All other parameters are endogenous. When used to solve a signal control problem (as in this paper), the capacity of the signalized lanes become endogenous, which makes the corresponding service rates, μ_i, endogenous.

5.2. Physical component used in Section 3.3

This model builds upon the model of Osorio and Bierlaire (2009) and of Osorio (2010, Chapter 4) (for its detailed derivation see Osorio and Chong (2015)). It approximates the traffic intensity of

queue i, ρ_i, by the effective traffic intensity, ρ_i^{eff}, where $\rho_i^{\text{eff}} = \rho_i(1 - P(N_i = k_i))$. It considers the System of Equations (38), and replaces ρ with ρ^{eff}. The following model is obtained.

$$\begin{cases} \lambda_i = \gamma_i + \dfrac{\sum_j p_{ji}\lambda_j(1 - P(N_j = k_j))}{(1 - P(N_i = k_i))} & \text{(39a)} \\ \rho_i^{\text{eff}} = \dfrac{\lambda_i(1 - P(N_i = k_i))}{\mu_i} + \left(\sum_{j \in \mathscr{D}_i} p_{ij} P(N_j = k_j)\right)\left(\sum_{j \in \mathscr{D}_i} \rho_j^{\text{eff}}\right) & \text{(39b)} \\ P(N_i = k_i) = \dfrac{1 - \rho_i^{\text{eff}}}{1 - (\rho_i^{\text{eff}})^{k_i+1}}(\rho_i^{\text{eff}})^{k_i}. & \text{(39c)} \end{cases}$$

6. SO algorithm

This SO algorithm is formulated in detail in Osorio and Bierlaire (2013) and is based on the derivative-free trust region algorithm of Conn et al. (2009a). The parameters of the algorithm are set according to the values in Osorio and Bierlaire (2013).

0. **Initialization.**

Define for a given iteration k: $m_k(x, y; \alpha_k, \beta_k, q)$ as the metamodel (denoted hereafter as $m_k(x)$), x_k as the iterate, Δ_k as the trust region radius, $\nu_k = (\alpha_k, \beta_k)$ as the vector of parameters of m_k, n_k as the total number of simulation runs carried out up to and including iteration k, u_k as the number of successive trial points rejected, ε_k as the measure of stationarity (norm of the derivative of the Lagrangian function of the trust region (TR) subproblem with regards to the endogenous variables) evaluated at x_k.

The constants $\eta_1, \gamma, \gamma_{inc}, \varepsilon_c, \bar{\tau}, \bar{d}, \bar{u}, \Delta_{max}$ are given such that: $0 < \eta_1 < 1$, $0 < \gamma < 1 < \gamma_{inc}$, $\varepsilon_c > 0$, $0 < \bar{\tau} < 1$, $0 < \bar{d} < \Delta_{max}$, $\bar{u} \in \mathbb{N}^*$. Set the total number of simulation runs permitted (across all points) n_{max}, this determines the computational budget. Set the number of simulation replications per point $\tilde{r}$ (here we use $\tilde{r} = 1$).

Set $k = 0, n_0 = 1, u_0 = 0$. Determine x_0 and Δ_0 ($\Delta_0 \in (0, \Delta_{max}]$).

Given the initial point x_0, compute $f_A(x_0)$ (analytical approximation of Equation (1)) and $\hat{f}(x_0)$ (simulated estimate of Equation (1)), fit an initial model m_0 (i.e., compute ν_0).

1. **Criticality step.** If $\varepsilon_k \leq \varepsilon_c$, then switch to *conservative mode*.

2. **Step calculation.** Compute a step s_k that reduces the model m_k and such that $x_k + s_k$ (the trial point) is in the trust region (i.e. approximately solve the TR subproblem).

3. **Acceptance of the trial point.** Compute $\hat{f}(x_k + s_k)$ and

$$\rho_k = \frac{\hat{f}(x_k) - \hat{f}(x_k + s_k)}{m_k(x_k) - m_k(x_k + s_k)}.$$

- If $\rho_k \geq \eta_1$, then accept the trial point: $x_{k+1} = x_k + s_k,\ u_k = 0$.
- Otherwise, reject the trial point: $x_{k+1} = x_k,\ u_k = u_k + 1$.

Include the new observation in the set of sampled points ($n_k = n_k + \tilde{r}$), and fit the new model m_{k+1}.

4. **Model improvement.** Compute $\tau_{k+1} = \frac{\|\nu_{k+1} - \nu_k\|}{\|\nu_k\|}$. If $\tau_{k+1} < \bar{\tau}$, then improve the model by simulating the performance of a new point x, which is uniformly drawn from the feasible space. Evaluate f_A and $\hat{f}$ at x. Include this new observation in the set of sampled points ($n_k = n_k + \tilde{r}$). Update m_{k+1}.

5. **Trust region radius update.**

$$\Delta_{k+1} = \begin{cases} \min\{\gamma_{inc}\Delta_k, \Delta_{max}\} & \text{if } \rho_k > \eta_1 \\ \max\{\gamma\Delta_k, \bar{d}\} & \text{if } \rho_k \leq \eta_1 \text{ and } u_k \geq \bar{u} \\ \Delta_k & \text{otherwise.} \end{cases}$$

If $\rho_k \leq \eta_1$ and $u_k \geq \bar{u}$, then set $u_k = 0$.

If $\Delta_{k+1} \leq \bar{d}$, then switch to *conservative mode*.

Set $n_{k+1} = n_k, u_{k+1} = u_k$, $k = k + 1$.

If $n_k < n_{max}$, then go to Step 1. Otherwise, stop.

7. Trust region subproblem

The considered SO problem is given by Equations (5)-(7). As described in Section 2.1, every iteration of the SO algorithm solves a metamodel optimization problem (Step 3a of Figure 1). The latter is also referred to as a trust-region subproblem. For a given iteration k, the problem is formulated as follows.

x	vector of green splits (i.e., decision variables);
$x(j)$	green split of signal phase j;
x_L	vector of minimal green splits;
x_k	current iterate at iteration k;
μ_d	service rate of lane d;
y	vector of endogenous macroscopic model variables;
q	vector of exdogenous macroscopic model parameters;
(α_k, β_k)	metamodel parameters at iteration k;
Δ_k	trust region radius at iteration k;
a_i	available cycle time of intersection i;
c_i	cycle time of intersection i;
e_d	fixed green time of signalized lane d;
s	saturation flow rate;
$\mathscr{P}_D(d)$	set of endogenous phase indices of lane d;
$\mathscr{I}$	set of intersection indices;
$\mathscr{I}(d)$	intersection index of lane d;
$\mathscr{P}_I(i)$	set of phase indices of intersection i;

$$\min_x m_k(x, y; q, \alpha_k, \beta_k) \tag{40}$$

subject to

$$\sum_{j \in \mathscr{P}_I(i)} x(j) = \frac{a_i}{c_i} \ \forall i \in \mathscr{I} \tag{41}$$

$$h(x, y; q) = 0 \tag{42}$$

$$\mu_d - \sum_{j \in \mathscr{P}_D(d)} x(j)s = \frac{e_d}{c_{\mathscr{I}(d)}} s, \ \forall d \in \mathcal{D} \tag{43}$$

$$\|x - x_k\|_2 \leq \Delta_k \tag{44}$$

$$y \geq 0 \tag{45}$$

$$x \geq x_L. \tag{46}$$

The objective function is the metamodel $m_k(x, y; q, \alpha_k, \beta_k,)$ (defined by Equation (3)). It is an iteration-specific approximation of the simulation-based objective function of Equation (5). Equations (41) and (46) are the signal control constraints, they correspond to Equations (6) and (7). The function h of Equation (42) represents the analytical macroscopic model. It represents, respectively, the System of Equations (38) for the case study of Section 3.2, and the System of Equations (39) for the case study of Section 3.3. Equation (43) associates the green splits of a phase with the flow capacity of the underlying lanes (i.e., the service rate of the queues). Constraint (44) is the trust region constraint, where Δ_k is the trust region radius. The endogenous variables of the queueing model are subject to positivity constraints (Equation (45)).

References

Abu-Lebdeh, G. and Benekohal, R. (1997). Development of traffic control and queue management procedures for oversaturated arterials, *Transportation Research Record* **1603**: 119–127.

Barceló, J. (2010). *Fundamentals of traffic simulation*, Vol. 145 of *International Series in Operations Research and Management Science*, Springer, New York, USA.

Barton, R. R. and Meckesheimer, M. (2006). Metamodel-based simulation optimization, *in* S. G. Henderson and B. L. Nelson (eds), *Handbooks in operations research and management science: Simulation*, Vol. 13, Elsevier, Amsterdam, chapter 18, pp. 535–574.

Batley, R. and Ibáñez, N. (2009). Demand effects of travel time reliability, *International Choice Modelling Conference*.

Ben-Akiva, M., Cuneo, D., Hasan, M., Jha, M. and Yang, Q. (2003). Evaluation of freeway control using a microscopic simulation laboratory, *Transportation Research Part C* **11**(1): 29–50.

Black, I. G. and Towriss, J. G. (1997). *Demand Effects of Travel Time Reliability*, Centre for Transport Studies, Cranfield Institute of Technology.

Branke, J., Goldate, P. and Prothmann, H. (2007). Actuated traffic signal optimization using evolutionary algorithms, *Proceedings of the 6th European Congress and Exhibition on Intelligent Transport Systems and Services*.

Bullock, D., Johnson, B., Wells, R. B., Kyte, M. and Li, Z. (2004). Hardware-in-the-loop simulation, *Transportation Research Part C* **12**(1): 73 – 89.

Carrion, C. and Levinson, D. (2012). Value of travel time reliability: A review of current evidence, *Transportation Research Part A: Policy and Practice* **46**(4): 720–741.

Cascetta, E., Nuzzolo, A., Russo, F. and Vitetta, A. (1996). A modified logit route choice model overcoming path overlapping problems: specification and some calibration results for interurban networks, *Proceedings of the 13th International Symposium on Transportation and Traffic Theory*, pp. 697–711.

Chen, C., Skabardonis, A. and Varaiya, P. (2003). Travel time reliability as a measure of service, *Transportation Research Record: Journal of the Transportation Research Board* **1855**(1): 74–79.

Chen, X., Osorio, C., Marsico, M., Talas, M., Gao, J. and Zhang, S. (2015). Simulation-based adaptive traffic signal control algorithm, *Transportation Research Board Annual Meeting*, Washington DC, USA. Available at: http://web.mit.edu/osorioc/www/papers/chenOsoNYCDOTtrbConf.pdf .

Chong, L. and Osorio, C. (2017). A simulation-based optimization algorithm for dynamic large-scale urban transportation problems, *Transportation Science* . Forthcoming. Available at: http://web.mit.edu/osorioc/www/papers/osoChoDynSOsubmitted.pdf .

Clark, S. and Watling, D. (2005). Modelling network travel time reliability under stochastic demand, *Transportation Research Part B: Methodological* **39**: 119–140.

Coleman, T. F. and Li, Y. (1994). On the convergence of reflective newton methods for large-scale nonlinear minimization subject to bounds, *Mathematical Programming* **67**(2): 189–224.

Coleman, T. F. and Li, Y. (1996). An interior, trust region approach for nonlinear minimization subject to bounds, *SIAM Journal on Optimization* **6**: 418–445.

Conn, A. R., Scheinberg, K. and Vicente, L. N. (2009a). Global convergence of general derivative-free trust-region algorithms to first- and second-order critical points, *SIAM Journal on Optimization* **20**(1): 387–415.

Conn, A. R., Scheinberg, K. and Vicente, L. N. (2009b). *Introduction to derivative-free optimization*, MPS/SIAM Series on Optimization, Society for Industrial and Applied Mathematics and Mathematical Programming Society, Philadelphia, PA, USA.

Department of Transportation (2008). Transportation vision for 2030, *Technical report*, U.S. Department of Transportation (DOT), Research and Innovative Technology Administration.

Dumont, A. G. and Bert, E. (2006). Simulation de l'agglomération Lausannoise SIMLO, *Technical report*, Laboratoire des voies de circulation, ENAC, Ecole Polytechnique Fédérale de Lausanne. Available at: http://web.mit.edu/osorioc/www/papers/dumont06BertRapport.pdf .

Flötteröd, G. and Osorio, C. (2017). Stochastic network link transmission model, *Transportation Research Part B* **102**: 180–209.

Fu, L. and Hellinga, B. (2000). Delay variability at signalized intersections, *Transportation Research Record: Journal of the Transportation Research Board* **1710**(1): 215–221.

Fu, M. C., Glover, F. W. and April, J. (2005). Simulation optimization: a review, new developments, and applications, *in* M. E. Kuhl, N. M. Steiger, F. B. Armstrong and J. A. Joines (eds), *Proceedings of the 2005 Winter Simulation Conference*, Piscataway, New Jersey, USA, pp. 83–95.

Gradshteyn, I. and Ryzhik, I. (2007). *Table of Integrals, Series, and Products*, Academic Press.

Gross, D., Shortle, J. F., Thompson, J. M. and Harris, C. M. (1998). *Fundamentals of queueing theory*, Wiley-Interscience.

Hachicha, W., Ammeri, A., Masmoudi, F. and Chachoub, H. (2010). A comprehensive literature classification of simulation optimisation methods, *Proceedings of the International Conference on Multiple Objective Programming and Goal Programming MOPGP10*, Sousse, Tunisia.

Hale, D. (2005). Traffic network study tool TRANSYT-7F, *Technical report*, McTrans Center in the University of Florida, Gainesville, Florida.

Hollander, Y. (2006). Direct versus indirect models for the effects of unreliability, *Transportation Research Part A: Policy and Practice* **40**(9): 699–711.

Jackson, W. B. and Jucker, J. V. (1982). An empirical study of travel time variability and travel choice behavior, *Transportation Science* **16**(4): 460–475.

Joshi, S., Rathi, A. and Tew, J. (1995). An improved response surface methodology algorithm with an application to traffic signal optimization for urban networks, *in* C. Alexopoulos, K. Kang, W. R. Lilegdon and D. Goldsman (eds), *Proceedings of the 1995 Winter Simulation Conference*, pp. 1104–1109.

Kamarajugadda, A. and Park, B. (2003). Stochastic traffic signal timing optimization, *Technical report*, Dept. of Civil Engineering, Center for Transportation Studies, Univ. of Virginia, Charlottesville, VA, USA.

Li, J.-Q. (2011). Discretization modeling, integer programming formulations and dynamic programming algorithms for robust traffic signal timing, *Transportation Research Part C: Emerging Technologies* **19**(4): 708–719.

Li, P., Abbas, M., Pasupathy, R. and Head, L. (2010). Simulation-based optimization of maximum green setting under retrospective approximation framework, *Transportation Research Record* **2192**: 1–10.

Li, Z., Hensher, D. A. and Rose, J. M. (2010). Willingness to pay for travel time reliability in passenger transport: A review and some new empirical evidence, *Transportation Research Part E* **46**(3): 384–403.

Little, J. D. C. (1961). A proof for the queuing formula: L= λ W, *Operations Research* **9**(3): 383–387.

Little, J. D. C. (2011). Little's law as viewed on its 50th anniversary, *Operations Research* **59**(3): 536–549.

Mahmassani, H. S., Hou, T. and Dong, J. (2012). Characterizing travel time variability in vehicular traffic networks: Deriving a robust relation for reliability analysis, *Transportation Research Record* **2315**: 141–152.

Mahmassani, H. S., Hou, T. and Saberi, M. (2013). Connecting networkwide travel time reliability and the network fundamental diagram of traffic flow, *Transportation Research Record* **2391**: 80–91.

Mathworks, Inc. (2011). *Optimization Toolbox Version 6. User's Guide Matlab*, Natick, MA, USA.

Mirchandani, P. and Soroush, H. (1987). Generalized traffic equilibrium with probabilistic travel times and perceptions, *Transportation Science* **21**(3): 133–152.

Newell, G. (1993). A simplified theory of kinematic waves in highway traffic, part I: general theory, *Transportation Research Part B* **27**(4): 281–287.

Ng, M., Kockelman, K. M. and Waller, S. T. (2011). A review of the correlation coefficient as a dependence modeling tool, *Proceedings of the Transportation Research Board (TRB) Conference*, Washington DC, USA.

Noland, R. B. and Polak, J. W. (2002). Travel time variability: a review of theoretical and empirical issues, *Transport Reviews* **22**(1): 39–54.

Odoni, A. R. and Roth, E. (1983). An empirical investigation of the transient behavior of stationary queueing systems, *Operations Research* **31**(3): 432–455.

OECD (2010). Improving reliability on surface transport networks, *Technical report*, Organisation for Economic Co-operation and Development.

Osorio, C. (2010). *Mitigating network congestion: analytical models, optimization methods and their applications*, PhD thesis, Ecole Polytechnique Fédérale de Lausanne.

Osorio, C. and Bierlaire, M. (2009). An analytic finite capacity queueing network model capturing the propagation of congestion and blocking, *European Journal of Operational Research* **196**(3): 996–1007.

Osorio, C. and Bierlaire, M. (2013). A simulation-based optimization framework for urban transportation problems, *Operations Research* **61**(6): 1333–1345.

Osorio, C., Chen, X., Marsico, M., Talas, M., Gao, J. and Zhang, S. (2015). Reducing gridlock probabilities via simulation-based signal control, *Transportation Research Procedia. 4th International Symposium of Transport Simulation (ISTS'14) Selected Proceedings*, Vol. 6, pp. 101–110.

Osorio, C. and Chong, L. (2015). A computationally efficient simulation-based optimization algorithm for large-scale urban transportation problems, *Transportation Science* **49**(3): 623–636.

Osorio, C. and Flötteröd, G. (2014). Capturing dependency among link boundaries in a stochastic dynamic network loading model, *Transportation Science* **49**(2): 420–431.

Osorio, C. and Nanduri, K. (2015a). Energy-efficient urban traffic management: a microscopic simulation-based approach, *Transportation Science* **49**(3): 637–651.

Osorio, C. and Nanduri, K. (2015b). Urban transportation emissions mitigation: Coupling high-resolution vehicular emissions and traffic models for traffic signal optimization, *Transportation Research Part B* **81**: 520–538.

Osorio, C. and Selvam, K. (2017). Simulation-based optimization: achieving computational efficiency through the use of multiple simulators, *Transportation Science* . Forthcoming. Available at: http://web.mit.edu/osorioc/www/papers/osoSelMultiModel.pdf .

Osorio, C. and Wang, C. (2017). On the analytical approximation of joint aggregate queue-length distributions for traffic networks: a stationary finite capacity Markovian network approach, *Transportation Research Part B* . Forthcoming. Available at: http://web.mit.edu/osorioc/www/papers/osoWangAggDisagg.pdf .

Osorio, C. and Yamani, J. (2014). Analytical and scalable analysis of transient tandem Markovian finite capacity queueing networks, *Transportation Science* . Forthcoming. Available at: http://web.mit.edu/osorioc/www/papers/osoYamDynAggDisagg.pdf .

Park, B. B. and Kamarajugadda, A. (2007). Development and evaluation of a stochastic traffic signal optimization method, *International Journal of Sustainable Transportation* **1**(3): 193–207.

Peterson, M. D., Bertsimas, D. J. and Odoni, A. R. (1995). Decomposition algorithms for analyzing transient phenomena in multiclass queueing networks in air transportation, *Operations Research* **43**(6): 995–1011.

Prashker, J. N. and Bekhor, S. (2000). Some observations on stochastic user equilibrium and system optimum of traffic assignment, *Transportation Research Part B: Methodological* **34**(4): 277 – 291.

Serafini, D. B. (1998). *A framework for managing models in nonlinear optimization of computationally expensive functions*, PhD thesis, Rice University.

Søndergaard, J. (2003). *Optimization using surrogate models - by the Space Mapping technique*, PhD thesis, Technical University of Denmark.

Stafford, R. (2006). *The Theory Behind the 'randfixedsum' Function*. http://www.mathworks.com/matlabcentral/fileexchange/9700.

Stevanovic, A., Stevanovic, J., Zhang, K. and Batterman, S. (2009). Optimizing traffic control to reduce fuel consumption and vehicular emissions, *Transportation Research Record* **2128**: 105–113.

Stevanovic, J., Stevanovic, A., Martin, P. T. and Bauer, T. (2008). Stochastic optimization of traffic control and transit priority settings in VISSIM, *Transportation Research Part C* **16**(3): 332 – 349.

Texas Transportation Institute (2012). 2012 Urban mobility report, *Technical report*, Texas Transportation Institute (TTI), Texas A&M University System.

Transport for London (2010). Traffic modelling guidelines. version 3.0, *Technical report*, Transport for London (TfL).

TSS (2011). *AIMSUN 6.1 Microsimulator Users Manual*, Transport Simulation Systems.

van Lint, J. W. and van Zuylen, H. J. (2005). Monitoring and predicting freeway travel time reliability: Using width and skew of day-to-day travel time distribution, *Transportation Research Record: Journal of the Transportation Research Board* **1917**(1): 54–62.

VSS (1992). *Norme Suisse SN 640837 Installations de feux de circulation; temps transitoires et temps minimaux*, Union des professionnels suisses de la route, VSS, Zurich.

Wong, S., Wong, W., Leung, C. and Tong, C. (2002). Group-based optimization of a time-dependent TRANSYT traffic model for area traffic control, *Transportation Research Part B* **36**(4): 291–312.

Yin, Y. (2008). Robust optimal traffic signal timing, *Transportation Research Part B* **42**(10): 911–924.

Yun, I. and Park, B. (2006). Application of stochastic optimization method for an urban corridor, *Proceedings of the Winter Simulation Conference*, pp. 1493–1499.

Zhang, C., Osorio, C. and Flötteröd, G. (2017). Efficient calibration techniques for large-scale traffic simulators, *Transportation Research Part B* **97**: 214–239.

Zhang, L., Yin, Y. and Lou, Y. (2010). Robust signal timing for arterials under day-to-day demand variations, *Transportation Research Record* **2192**: 156–166.